CHAPTER 10 ROOF/RIB FALLS, AND FLOOR HEAVES

10.1 INTRODUCTION

An underground entry or opening is surrounded by rock strata on the roof and bottom and coal pillars on both sides. Hence the issues of entry stability consist of stability of roof, floor, and pillars. Pillar stability ranges from rib sloughing to complete pillar collapse. This chapter will address roof falls, rib sloughage, and floor heaves. Pillar collapse is discussed in Section 5.8 (p. 270).

10.2 ROOF FALLS

10.2.1 Introduction

Roof falls are the unintended fall of rock from the mine roof. They are a common problem in U.S. underground coal mines where roof bolts are the sole means of roof reinforcement. Every roof fall leaves an open cavity where the fallen rock debris dropped to the floor. The debris must be cleaned up and the open cavity must be re-supported if the opening is to be used further.

Roof falls can be sudden, or they may take time to develop before their final fall. The causes of various types of roof falls are not fully known. Cutter roofs are best known in the industry and most studied by researchers.

There are indications that as roof bolting technology advances and geological conditions get worse, roof fall characteristics are also changing, i.e., the size of roof falls are getting bigger and bigger.

10.2.2 Types of Roof Falls

Several methods have been proposed for classification of roof falls. Connolly (1970) classified roof falls into three types based on the time interval between active mining and roof fall, conditions of stress build-up in the roof, and the modes of roof fall. Shepherd and Fisher (1978) also listed three types of roof falls, those from good roofs with little or no fall; those from troublesome roofs, such as scaly or heavy roofs with low cutter falls and wide flat roof falls; and those from severely failed roofs which are usually very heavy with high cutter fall, and dome falls.

Patrick and Aughenbaugh (1979) classified roof falls into two types, regular and irregular, based on the geometry and size of the roof fall. The regular type includes dome and arch falls, whereas the irregular type includes minor and sloughing or rashing. The dome fall occurs mostly at four-way intersections, while the arch fall generally spans a length more than one combination of an intersection and an entry between pillars.

Wier (1970) described six types of roof falls as controlled by different combinations of geological effects: (1) dust roof falls less than 1 ft (0.3 m) thick; (2) lenticular roof falls between two sandstone rolls; (3) ironstone concretion falls by gravity; (4) slate roof falls due to the fissionable black shale breaking in large slabs along a bedding plane or parting; (5) clay vein falls; and (6) massive roof falls more than 20-30 ft (6.1-9.1 m) high.

Smith and Szwilski (1985) stated that the basic geometry or shape of a roof fall depends greatly on the stresses placed on the roof and floor. They classified all roof falls in Appalachia into three categories: dome, arch, and laminar-shaped roof falls. Laminar- and dome-shaped falls are attributable to the results of tensile stresses and associated geological features or

defects in the roof strata. The difference between dome- and laminar-shaped falls is the location of the intersection of the separation planes. If the separation planes intersect on a bedding plane, laminar roof falls may develop; if the separation planes intersect inside a bed, a dome-shaped roof fall may develop. Arch-shaped roof falls are similar to dome-shaped except their side edges are straight.

Moeb and Stateham (1985) divided roof failure into two types: stress and geologic effect. Stress effect is further divided into (1) valley effect attributable to a narrow and sharp valley at the surface; (2) regional stress effect due to large lateral compressive stress; (3) induced stress interaction effect due to stress concentration induced by the extraction of an overlying or underlying seam. The geologic effect is subdivided into four types: (1) weak, soft, and poorly laminated immediate roof; (2) immediate roof sensitive to moisture; (3) thinly-laminated immediate roof; and (4) minor structure, such as slickensides, kettlebottoms, clay veins, and concretions.

Peng (2007) stated that roof falls are rare in strong roof such as sandstone and limestone, except when those rocks contain abundant fossils and other foreign materials or with poor cementing materials, and that roof falls occur mostly in shale roof and can be classified into two types: skin falls and entry falls (Fig. 10.2.1). **Skin falls** are failure of rock strata between two adjacent bolts or between two rows of bolts, 1-3 ft (0.3-0.91 m) high (Bauer et al., 1999; van der Merwe, 2001). **Entry falls** refer to those with their cavities covering the whole entry width or a large part of the entry. Their heights cover a great part of the roof bolts or frequently are higher than the bolting horizon.

A B

Fig. 10.2.1 Two types of roof falls: A, skin fall, and B, entry fall (Peng, 2007)

Skin falls occur mainly in rock strata sensitive to weathering. They may develop into entry falls if proper supports are not installed in a timely manner. Entry falls can further be divided into two types. In the first type, the roof strata are weak and very thick (or thicker than the bolting horizon). The whole roof shears off vertically along the pillar rib on one or both sides all the way up above the bolting horizon. In the second type, the strata, either the same or different types in varying thickness, are bedded and stiffer. Each layer or combination of layers behave independently in that the lowest beam is the longest and breaks right above the ribs. The second lowest beam breaks some distance away from the ribs, i.e., its beam length is shorter than the lowest beam (Fig. 10.2.2). This process repeats layer by layer upward, eventually forming a dome shape cavity after these beams have fallen down. Therefore, bedding planes or laminations play an important role in the deformation of roof strata. Very

often, bedding planes or laminations act as sliding planes, even though they look extremely tight. Sliding along these planes often precedes failure of the intact materials between bedding planes or laminations.

A B

Fig. 10.2.2 Entry fall: A, inby wall of the roof cavity, and B, beam structures of the right edge of the roof cavity shown in A (Peng, 2007)

10.2.3 Roof Fall Accident Characteristics

There are two major sources of roof fall data. The first one is the official roof fall fatalities report and the second one is the roof fall data reported to MSHA by the mine operators as required by law.

Biswas and Zipf (2003) examined the rock-fall-related incident narrative available from the MSHA database covering a period from 1984 to 1999. They found six major categories of root causes for rock falls: support system failure due to inadequate or improper spacing (11.9 %) and fall between shields (3.5 %), operating a miner (10.1 %), scaling roof (9.6 %), drilling or bolting (8.4 %), rib roll or slough off (8 %), and setting timbers or cribbing (4.7 %) (Table 10.2.1). These findings were largely supported by Bauer et al., (1999), who examined the injury-fatalities data due to roof and rib skin failures from 1993 to 1997 and classified roof falls into skin or massive failures based on the thickness and areal extent of the fallen material. Roof skin failures were less than 2 ft (0.6 m) thick, while the rib skin failures were less than 3.5 ft (1.1 m) thick. A similar definition was used by Tadolini and Dolinar (2001).

The six top-ranking causes listed in Table 10.2.1 clearly indicate the contributions of ground characteristic, support characteristics, and human factors for a given accident. The rank order of these top root causes varies somewhat from year to year.

The volume of broken rock involved in the injury-incident was mostly larger than 1 ft^3 (0.03 m^3), and 40 % of them involved less than 1 ft^3 (0.03 m^3).

Van der Merwe (2001) investigated a total of 182 roof falls in South Africa and found that the causes of roof falls differed for different thickness ranges of roof falls. The thin or skin falls, which accounted for 70 % of all fatalities, were predominantly caused by ineffective joint support and excessive bolt spacing. Ineffective joint support was found to be a predominant cause for all thickness ranges and the influence of excessive bolt spacing diminished with increasing fall thickness.

Table 10.2.1 Ranking causes for ground fall incidents (Biswas and Zipf, 2003)

Rock mass failure		Support system failure		Human activity factors	
Type	%	Type	%	Type	%
Other weakness	39.7	Inadequate or improper spacing	11.9	Operating a miner	10.1
Rib-roll or slough-off	8.0	Fall between shields	3.5	Scaling down	9.6
Rockburst	2.1	Inadequate maintenance	0.1	Drilling or bolting	8.4
Joint planes or bedding planes	<0.1	Inadequate bolt length	<0.1	Setting timbers or cribbing	4.7
Excessive span	<0.1			Mucking	1.7
Total	50.0	Total	15.5	Total	34.5

10.2.4 Roof Falls at Intersections

1. Characteristics

There are two types of intersections: three-way and four-way. Intersections can be formed by either entry and crosscut perpendicular to each other, or the entry and crosscut intersect at a certain angle convenient to face equipment operation. Intersections may be aligned in a straight line in multiple entry development, or they may be staggered for better roof stability. Four-way intersections with entries and crosscuts perpendicular to each other and aligned in a straight line are by far the most popular type.

All roof fall statistics and studies (Peng, 1986, 1997, and 1999) showed that a great majority of roof falls were located at intersections of entries and crosscuts. The major reason is that the span width of an intersection, which is represented by either the diagonal distance between two opposite corners or the sum of the entry width and crosscut width, is much larger than the width of an entry/crosscut between pillars.

In most mines, the roof bolting systems employed for intersections are the same as those used for entries/crosscuts between pillars. In some cases, special roof bolting patterns are employed for intersections. The most popular practices are to decrease the roof-bolt spacing 1 ft (0.3 m) less or to increase the bolt length 1-2 ft (0.3-0.61 m) longer than those employed in the entries between pillars (Stahl, 1962). These generalized practices certainly are not applicable to all geological and mining conditions. Similarly, three-way intersections, although more difficult to develop, are adequate for medium and stable roofs, but inadequate for weak roof (Peng and Park, 1977a).

Numerical modeling indicated that tensioned bolting at the intersections provides beam-building effect within 3 ft (0.9 m) of the roofline and suspended the bolted strata below the anchorage horizon. Therefore, the bolts must be longer than those used in entry and crosscut. Also bolt density must be increased near the intersection corners (Zhang and Peng, 2003b).

A collection of 22 intersection roof falls in the Pittsburgh seam showed the following dimensional relationship of roof fall cavities at intersections (Peng, 1986),

$$H_t = 0.37\,(D_{max}\,D_{min})^{1/2} \tag{10.2.1}$$

where H_t is roof fall height, and D_{max} and D_{min} are the maximum and minimum dimensions of the bottom cross-section of the roof fall cavity.

MSHA roof fall data (Molinda et al., 1998) showed that intersections are, on a foot by foot basis, about 8-10 times more likely to have roof falls than entries/crosscuts; that a four-way intersection is 1.28 times more likely to have roof falls than a three-way intersection; that for weak roofs, roof fall rates increase with increasing roof span; and that various roof fall rates are associated with different types of roof supports installed. Vervoort (1990) found similar statistics in South Africa, and in addition, fatal falls in roadways are on average larger than those at the face.

Due to their large spans, the adverse effect of geological anomalies tended to be magnified at intersections. Slips (Bugden and Cassie, 2003) and stacking slickensides (Peng et al., 2007a) have been found to have contributed to roof falls at intersections.

2. Supporting Methods

Finite element computer analysis (Peng and Okubo, 1978a and 1978b) showed that the minimum bolt length for four-way intersections should be at least one half the entry width at the center area of the intersection and from 0.4 times to one full entry width long for three-way intersection, depending on the angle between the entry and crosscut.

Figure 10.2.3A shows the potential failure mode at an intersection (Singh et al., 1998). Cutters (gutters) occur in a 1.64-2.3 ft (0.5-0.7 m) wide strip parallel to the rib edge. Sliding type failure occurs between 0.2 W_o and 0.4 W_o (W_o is opening width) from the opening centerline. Dome or arch failure covers the entire width of the entry and extends to a height of (0.5-1.0) W_o. Consequently there are three zones of stability. Zone I represents typical roof conditions that exist between pillars. Zone II experiences increased strata loading by some 20%, requiring longer bolts with closer spacing and increased load ratings. Zone III requires bolt lengths 50% longer than those in zone II with corresponding increased load-bearing capacity (Fig. 10.2.3B).

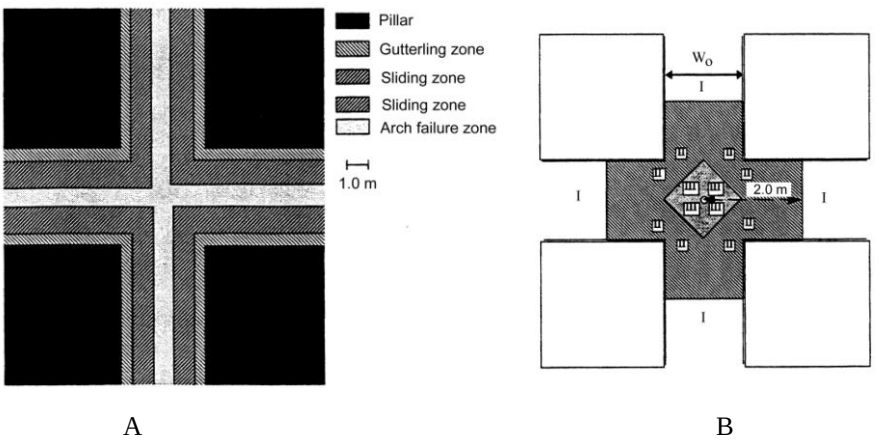

Fig. 10.2.3 Location of various modes of failures (a) and zones of instability at four-way intersection (Singh et al., 1998)

In recent years, for intersections with weak roof, supplementary supports, mainly one or more cable bolt, 8-10 ft (2.4-3.1 m) and 12-16 ft (3.7-4.9 m) long, have been successfully used

for room-and-pillar mining and longwall gateroads, respectively. The reason that those long cable bolts have been so successful is that they can reach beyond the zone of movement created by the excavation of an opening and anchored at the virgin roof strata.

10.2.5 Causes of Roof Falls

Many roof falls have been attributed to high horizontal stresses (Keim and Miller, 1999; Agapito et al., 2005). For more detail discussion about roof falls, see Sections 6.2, (p. 299), 6.3 (p. 303), and 10.3.2 (p. 477).

In recent years, many roof falls have been found to be related to roof rock of poor quality (Peng, 2007). Many roof falls, including cutter roofs, do not occur in massive, strong roof, such as sandstone and sandy shale. Rather, they occur in weak roofs. A "**weak**" roof is not restricted to those rocks that have a low uniaxial compressive strength (UCS) as determined in the laboratory. Stack rock accounted for the majority of massive and ugly roof falls. **Stack rock** is thin layers of sandstone or sandy shale interbedded with thin films of carbonaceous (black) materials (Fig. 10.2.4). The thicker the total thickness, the worse it makes a roof. Its UCS, as determined by the current testing standards in the laboratory, does not represent its behavior underground. Stack rock, being composed of sandstone or sandy shale, have high UCSs. But underground, the thin films of carbonaceous materials are where stack rock breaks easily into slabs. The thinner the sandstone/sandy shale layers and the denser the thin films of carbonaceous materials, the sooner and worse the roof will fall. For this type of roof strata, stability tests of thin beams or cantilevers are more representative, not the UCS as conventionally obtained from standard rock mechanics tests.

Another weak roof that appears to be contrary to the strength obtained in the laboratory is laminated clayey shale. When it is dry, under which the laboratory strength is determined by following the current prevailing testing standards, its strength is high, thereby normally projecting a stable roof. But once they are exposed underground and subject to the wet and dry annual cycles of the ventilation air, their laminations become active and rock materials begin to crumble. The larger the clay content, the sooner and worse the roof will fall. For this type of rock, its sensitivity to weathering (moisture) is the most important property for stability evaluation, not the conventional UCS (see section 10.5, p. 486)

10.2.6 Re-supporting the Roof Fall Area

Re-supporting the roof fall area is a difficult, dangerous, and expensive task (Beerbower, 1985; Chlumecky, 1981), because it must be performed in compliance with the law requiring that persons must work under adequate temporary supports beyond the last row of permanent roof supports. In most roof falls, the fall edges are sloped and irregular, making it difficult to erect a floor-to-roof temporary support. If the roof fall is high, the supporting capacity of tall and slender posts and jacks is greatly reduced. Furthermore, they are easily knocked out of place by the clean-up machines. A good re-support procedure requires that it works in proper sequence (Stears et al., 1976) from the supply end step by step into the fall area, i.e., barring down loose materials, testing the roof, setting up temporary supports, and finally, installing permanent supports.

With the popular use of remote control, clean-up of fall debris with a continuous miner has become easier and safer. The fall material can be cleaned up either before or after the supports are installed, whichever is convenient. Frequently, fall debris is used as stages for installing roof supports.

Fig. 10.2.4 Stack rocks. Arrows indicate thin film of carbonaceous materials. b is broken roof bolt, R is roof bolt, and bh is bolthole (Peng, 2007)

There are several methods of re-supporting the roof. The most common one is to bar down all the loose pieces and re-bolted with roof bolts. The roof-bolting system can either follow the original pattern or create a denser pattern (often irregular) with stronger and longer bolts. This method requires that the roof bolter be able to reach the top surface of the roof fall cavity.

If the roof falls are shallow, cribbing is erected on top of the three-pieced steel (I-beam) set or simply using the three-pieced steel sets properly spaced and strutted between the sets.

For very high roof falls, arch canopy is used (Peng, 1986). An arch canopy must be designed for protection against subsequent roof falls that may cause the canopy to collapse. According to Allwes and Manglsdorf (1986), 87 % of all rehabilitation accidents were due to falls involving less than 20,000 ft-lbf of energy per foot length of the roof fall. When a slab of rock, W, falls on the arch canopy (Fig. 10.2.5A), the gross energy available for deforming the arch is equal to the loss of potential energy of the rock slab, i.e., the arch must be designed to withstand a gross energy equivalent to

$$E_g = W\,(H - h_p) \tag{10.2.2}$$

where W is the weight of the rock slab (lbf/ft), H is the void height or height of roof fall, (ft), and h_p is protection height (ft). E_g is not a constant, but increases as H increases and W decreases (Fig. 10.2.5B).

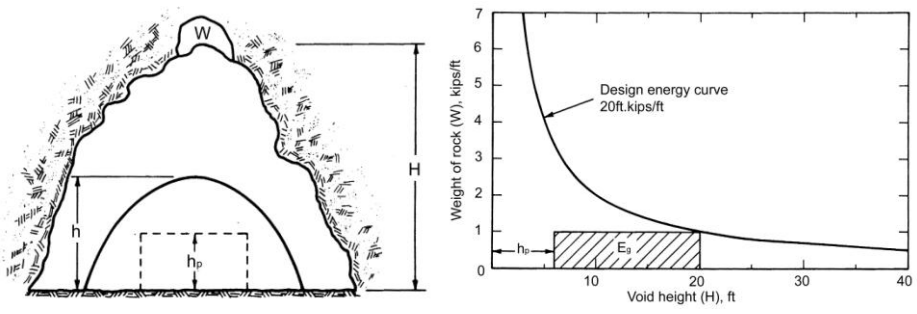

Fig. 10.2.5 Design criteria for an arch canopy: A, dimensions and B, energy curve (Allwes and Mangelsdorf, 1986)

It must be emphasized that in addition to safety issues, the cost of cleaning up and re-supporting a roof fall is very high. Therefore, it pays to have a well-designed roof control plan to prevent or reduce roof falls.

10.2.7 Polyurethane Injection

Polyurethane injection is widely used to stabilize adverse roofs, either to prevent further deterioration of existing adverse roofs or to strengthen the expected adverse roof in advance of mining, especially longwall mining where any downtime events causing production delays are very costly (Fig. 10.2.6) (Peng, 2006). Polyurethane injection fills out voids, reduces the rate of roof displacement and extension of weak zones, and increases cohesion and frictional resistance of strata (Frith et al., 2003).

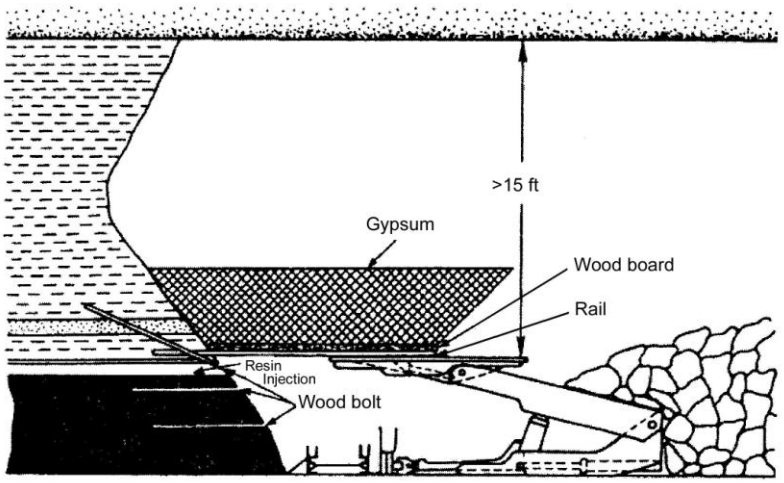

Fig. 10.2.6 False roof built to pass through a very large roof fall (Peng and Chiang, 1984)

The polyurethane binder system consists of two components, component A (a polymeric isocyanate) and component B (a polyol resin) (Popovich et al., 2001). They are mixed and injected under pressure into the rock strata through drill holes using specially developed equipment (Fig.10.2.7A). The mixed components enter the strata through the mixer/packer unit, fill the voids between the packer and the end of the hole (Fig. 10.2.7B), and proceed to flow into the rocks through fractures and bedding plane separations. The largest cracks that offer the least resistance are filled first, followed by smaller fractures. The result is that the rock strata are restored to their intact condition. The flow direction of the binder's migration within the strata can sometimes be changed, and leaks that appear on the rock's surface can be restricted. The injection holes are typically 1-3/8 in. (34.9 mm) in diameter on 10 ft (3.04 m) spacing.

Under laboratory conditions, the mixed components cure in two minutes. At that point, rock strata are thought to begin to consolidate. But underground, the mixed components should be allowed to cure for at least two hours, after which the binder system should offer adequate support to enable mining to proceed. In eight to 10 hours, the binder should have reached its ultimate strength. The final rock binder has a uniaxial compressive strength (UCS) of 10,200 psi (70.34 MPa), uniaxial tensile strength (UTS) of 3,850 psi (26.5 MPa), and maximum elongation of greater than 17 percent at ultimate strength.

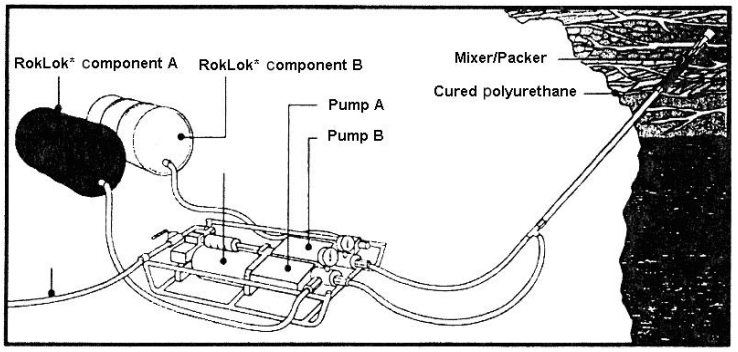

A

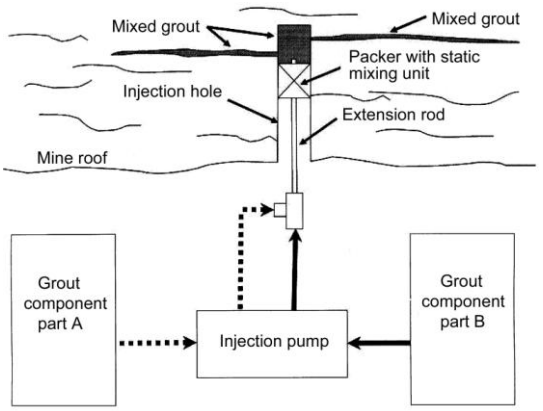

B

Fig. 10.2.7 Polyurethane injection system: A. (Popovich et al., 2001), B. (Monaghan and Trevits, 2004)

J Wang et al., (1996) reported that polyurethane hard plastic foam is produced by the reaction between two components of polyisocyanate and polyether. During the chemical reaction, CO_2 is produced, making the polyurethane foam swell and solidify rapidly. The polyurethane materials have a foaming time of 2-6 minutes, gel-time of 1-25 minutes, cohesive strength 127.6 - >391.5 psi (0.88 - >2.7 MPa), and compressive strength 277-1,145.5 psi (1.91-7.9 MPa). During the chemical consolidation for the fractured rocks, the liquid materials diffuse, coagulate, fill up the fractures, and form a diffusion radius ranging from 1.64 to more than 10 ft (0.5 to >3 m) (Fig. 10.2.8).

Successful strata consolidation depends on locating fractured rocks and their areas of extent and fracture density. For roof reinforcement, vertical holes are used. For longwall faces, injection drill holes oriented at 10^o to 20^o from horizontal (Fig. 10.2.6) and strategically located at the coal seam/roof interface are recommended. The location, pattern, spacing, depth, and quantity of components for the injection holes require perceptive judgment from a person(s) knowledgeable in both behavioral characteristics of the roof and the injection system. The amount and rate of polyurethane injection at each hole varies, depending on the site condition and practitioners. Polyurethane injection may be terminated when certain back pressure develops or injection causes excessive roof dilation (e.g., > 0.16 in. or 4 mm) (MacPherson and Payne, 1999).

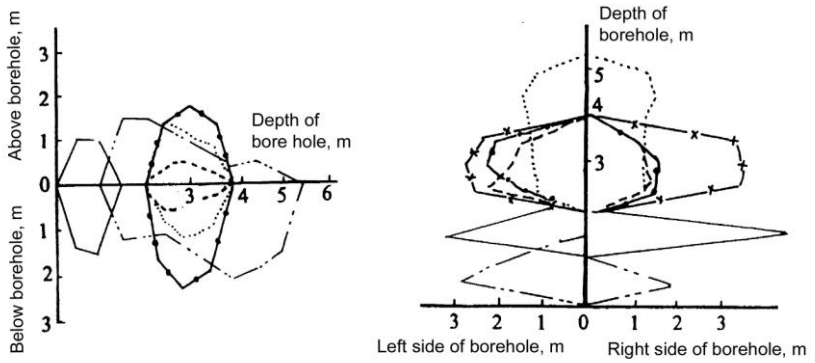

Fig. 10.2.8 The diffusion radius of polyurethane consolidation (J Wang et al., 1996)

For best results, the temperature should be equal to or greater than 60° F (16° C). Normal operating pressure measured at the injection pump should be around 400 to 800 psi (2.76-5.52 MPa). Resistance to flow in the pumps, hoses, and mixer/packer accounts for 80-90 percent of the total pressure. In order to overcome additional hose extension, the recommended operating pressure is 700 to 1,100 psi (4.83-7.59 MPa).

A classic example of a polyurethane application to stabilize the roof was described by McCabe (1981). When the coal seam was 15 ft (4.6 m) or more, the roof was stable. When the seam split, the roof was unstable. A roof crack along the longwall face was 200 ft (61 m) long, causing a detached block, 15 x 20 x 175 ft (4.6 x 6.1 x 53.3 m), to rest on the chock supports. After injection with polyurethane, the roof bent and settled down gradually in one piece in the gob.

In Germany, procedures have been established in the use of strata injection as a means of stabilizing brittle and heavily stressed ground as well as faulted zones. Tests are available for determining the injection capacity of the strata and the operating characteristics and workability of the injection product. A proper combination of injection products and equipment must be selected in order to ensure that the operation will be a success (Bolesta and Ruppel, 2001).

10.2.8 Prediction of Roof Falls

Conventionally, a sounding bar with a blade or a walking stick with a rounded metal head is used to identify loose roofs by tapping on the surface of the rock (see the statue of the dust cover). A "sharp" sound indicates a **solid roof**, whereas a "drummy" sound indicates a **loose roof**. This method is qualitative and cannot reveal the size and depth of the loose rock slabs. To quantify this method, tests performed by Repsher (1991) showed that the ratio of energy contained in two frequency bands (500-1,000 Hz and 3,000 to 3,500 Hz) can be used to indicate the degree of detachment for the rock in question. Solid rock has an energy ratio between 0 and 10, while loose rock blocks have an energy ratio between 20 and 40.

A roof-to-floor convergence meter (Bauer and Chekan, 1981; Shepherd and Chaturvedula, 1992) or tell-tale devices (Bigby et al., 2003) have also been used to monitor roof movement. Roof convergence under normal roof conditions would be small and steady, but it accelerates rapidly immediately before a roof fall with warning time on the order of 5 minutes (Fig. 10.2.9). However, due to the vast area to be covered in an underground mine, or

even a particular working section, the number of the stations and labor required for monitoring are often impractical to implement. Therefore, Iannacchione et al., (2004) recommended using roof convergence measurement in conjunction with microseismic monitoring. In this approach, immediately after the microseismic method determines the approximate location and time of roof falls, convergence stations are then properly deployed for last stage monitoring.

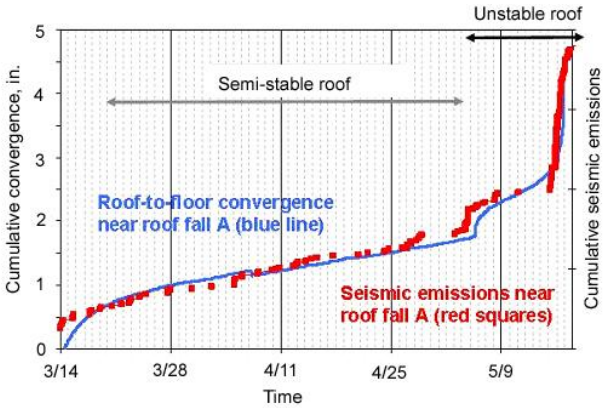

Fig. 10.2.9 Comparison between roof convergence, microseismic event frequency, and local stability conditions (Iannacchione et al., 2004)

Maleki (1990) developed empirical failure criteria for roof stability based on 200 field measurements of rock mass stability in 8 mines. Roof strata deform 1-14 in. (25.4-355.6 mm) prior to failure, depending on rock mass properties and pillar stiffness. Failure of roof strata occur when roof movement rate accelerates to a critical limit, stabilizes for a short time, and then accelerates again, resulting in roof collapse. Time-to-caving varies from 1 minute to 10 days (Table 10.2.2).

Table 10.2.2 Critical roof movement rate and time-to-caving (Maleki, 1990)

Rock/pillar type	Critical rate , in./day	Time-to-caving , day
Brittle rock and stiff pillar	0.024-0.04	2-10
Brittle rock and yielding pillars	0.2-0.3	1-90
Viscoelastic roof and viscoplastic pillars	1	No roof fall

In pillar extraction using MRSs, roof falls occur when (1) roof movements accelerate, reaching critical limits of 0.2 in./min (5 mm/min); (2) a high potential for roof-pillar failure exists when the MRS loading rate increases beyond 10,000 lbf/min (44 KN/min); (3) roof-pillar instability exists when the MRS loading rate is 5,000-10,000 lbf/min (22-44 KN/min); and (4) roof-pillar is stable when the MRS loading rate is smaller than 5,000 lbf/min (22 KN/min) (Fig. 10.2.10) (Maleki et al., 2001).

Microseismic techniques have been used to predict longwall gob caving (Iannacchione et al., 2005; Srinivasan et al., 2005) and roof falls (Iannacchione et al., 2001). Rock fracture begins with cracks that initiate, propagate, and coalesce, leading to final rupture. Stress waves are generated at each stage of the fracture process. By monitoring the magnitude and density of the stress waves, which is commonly referred to as **acoustic emission**, it is possible to estimate

the impending failure. For more details of the application of microseismic techniques for emission source location, refer to Section 9.6 (p. 455).

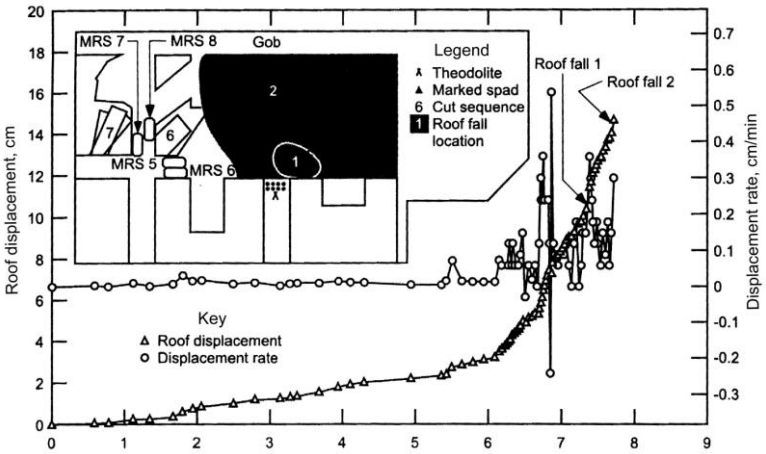

Fig. 10.2.10 Roof displacement history prior to roof falls (Maleki et al., 2001)

Iannacchione et al., (2001) monitored the failure characteristics of roof falls at an underground stone mine. They found that roof falls are preceded by a period of accelerating microseismic events and identified 1,394 background events of microseismic activity occurring at a rate ranging from 0.14 to 0.35 events/hour. The duration of individual roof rock failures ranged from 5-40 hours. Therefore, they concluded that significant relationships exist between the intensity of the microseismic activity and the scale of the roof failures, and that microseismic activity associated with roof falls occurs in distinct forms with the final failure event occurring during approximately a 12-hour period.

Iannacchione et al., (2005) analyzed the microseismic data associated with gob caving in longwall mining where the main roof of conglomerate was 98.4-114.8 ft (30-35 m) thick lying about 5.2 ft (1.6 m) above the seam roof top. The striking feature relating to the caving of conglomerate is that seismic activity generally increases dramatically close to the time of roof falls. For example, Fig. 10.2.11 shows seismic activity remains at a relatively constant rate until a short time before the roof fall. Microseismic activity was associated with the initiation and development of the stepped failure surface of the caved zone, with the accelerating rate of seismic activity signaling the completion of the stepped face. The seismic alarm criteria consisted of four sub-criteria: (1) frequency 1 (F1) - when 6 or more seismic events occurred in a 10-second period; (2) frequency 2 (F2) - when 5 multiple events (i.e., more than one distinct signature per record) occurred in one minute; (3) magnitude - when more than one event with a moment magnitude, which is approximately similar to the Richter scale, larger than -1.0 in a 2 minute period; and (4) trend – interpreted trends of seismic activity such as apparent volume and the energy index. These criteria produced an average forecast time of 54 minutes, 12 minutes better than that forecasted by employing shield leg pressure and audible noises.

Srinivasan et al., (2005) monitored the caving of a thick-bedded sandstone above a narrow longwall panel, 492 ft (150 m) wide and 243 ft (74 m) deep. In general, microseismic activity increased with the advance of the face and became low when mining stopped. The reported roof falls took place after 2-6 hours of microseismic event rate attaining the peak value, followed by a sharp decrease to 10-12 % of the peak value (Fig. 10.2.12 upper).

Microseismic events showed the initiation, and propagation of fractures that ultimately resulted in roof falls. Thus it was possible to map the fractures in 3-dimensions in the roof layers as the longwall face retreated (Fig. 10.2.12 lower).

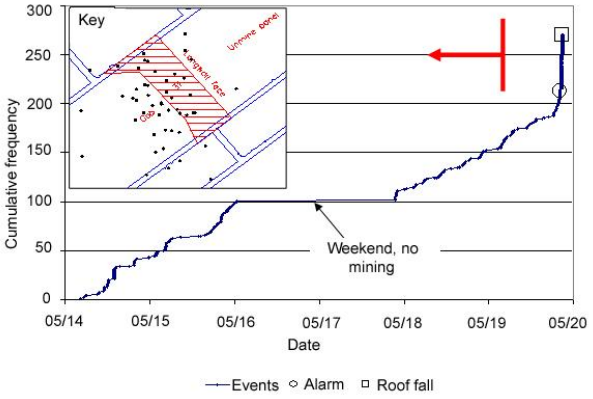

Fig. 10.2.11 Cumulative frequency of seismic events associated with roof fall (Iannacchione et al., 2005)

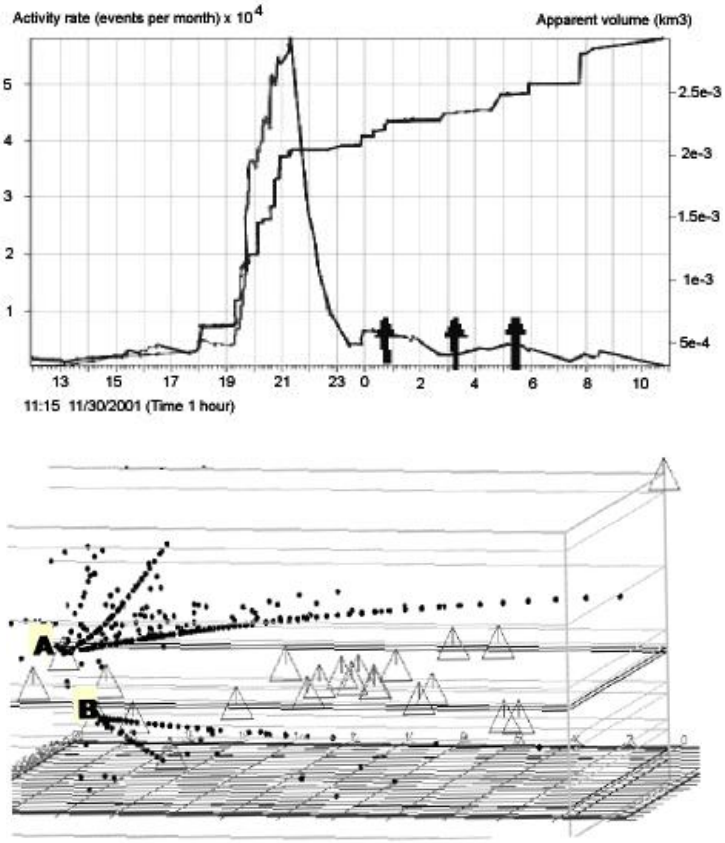

Fig.10.2.12 Upper, microseismic event rate versus apparent volume of a roof fall; lower, distribution of microseismic activity plot on the 3-D section of the mine (Srinivasan et al., 2005)

10.2.9 Time Lapse between Roof Exposure and Bolt Installation

There is a common belief that the roof should be bolted as soon as it is undermined, because the longer time lapses between undermining and bolt installation, the larger the roof deflection and the more damage the roof suffers. A larger roof deflection usually involves bed separation or de-lamination of laminated strata or both. So if the roof is strong, the continuous miner can make a deeper cut. Conversely, a shorter cut is necessary to keep the roof up. Deeper cuts speed up development and increase productivity.

There are conflicting reports regarding whether the time lapse between undermining and support installation affects roof stability (Radcliffe and Stateham, 1980; Maleki et al., 1994). Radcliffe and Stateham (1980) monitored roof convergence in Bear Mine of Somerset, CO, where the shale roof, 3-20 ft (0.9-6.1 m) thick, was intensely fractured and slickensided. The measured displacement in cuts that were left unsupported over time intervals of 15 minutes to more than 12 hours indicate that time lapse does not influence the stability of the roof after support. Therefore time lapse is not a critical factor in roof stability for this mine, provided permanent support is installed before the roof falls.

Maleki et al., (1994) monitored the roof movement and bolt loads of a mine located near Rangely, CO, where the roof consisted of thinly-bedded siltstone and massive fine-grained siltstone. They compared roof movement and bolt loads between two different entry development procedures. In the conventional method, the bolts were installed after the box cut of 10 ft (3 m) wide by 18 ft (5.5 m) deep was completed. In the alternative method, the box cut was 12 ft (3.6 m) wide by 10 ft (3 m) deep. The results showed that the alternative method had 23 % improvement in roof fall volume per crosscut advance and 15 % improvement in roof deformation. Monitoring of 15,200 mechanical bolts in a western mine showed that roof sag increases with time lapse between mining and bolt installation (Brest van Kempen et al., 1986; Maleki et al., 1986).

Therefore, it appears that the effect of time lapse between undermining and bolt installation depends on site specific geological conditions.

10.3 CUTTER ROOFS

10.3.1 Introduction

Cutter roofs or simply **cutters** refer to the fractures that occur at the upper corners (i.e., the intersection between the roof line and pillar rib line) of a rectangular entry or opening (Peng, 2007). Cutters range from less than 1 in. (25.4 mm) long and a few tenths of an inch (several millimeters) wide at the initiation stage to more than 100 ft (30.5 m) long and a few feet wide immediately before a massive roof fall (Fig. 10.3.1). They tend to propagate vertically or near vertically upward from one or both upper corners of an entry (Fig. 10.3.2). When the fracture extends to a height above the roof-bolt anchorage horizon and/or breaks along a weak bedding plane, a massive roof fall occurs.

Cutters have been found to have been formed ahead of, immediately after, or long after, an entry development. They may occur on the right or left side of the rib exclusively; they may occur on the right side first and then move to the left side or vice versa. They may form only in the entry or crosscut exclusively, or they may switch from entry to crosscut or vice versa (Peng, 2007).

Cutters do not always lead to roof falls. Many cutters stayed the same throughout the whole entry/crosscut life as they were found, while others progressed to various stages and stopped. The rate of propagation of cutters from stage to stage also varies (Peng, 2007).

Cutters have long been known to be associated with rectangular openings (Roley, 1948) and attributed to high lateral pressure (Phillips, 1947) or rock type (Thomas, 1950). They are more prevalent in the eastern and central coal fields, due mainly to weaker immediate roofs. Despite widespread occurrence, the complex mechanisms involved in cutter roof development were not unraveled until the late 1970s to mid 1980s (Hill, 1986; Hill and Bauer; 1984; Iannacchione et al., 1984; Kripakov, 1982; Nicols, 1978; Su and Peng, 1985).

A

B

C

Fig. 10.3.1 Cutters at various stages: A, initial stage showing only fracture lines, B, advanced stage showing roof skin peeling off, and C, small roof falls along the roof- pillar corner (Peng, 2007)

It is generally believed that cutter roof is caused by the shear stress at the entry corner being larger than the shear strength. The high shear stress at the entry corners results possibly

from a large overburden weight and/or high horizontal stress at the ribs. However, high vertical and horizontal stresses are not the only factors contributing to cutter roof development. Other factors such as local geology, larger topographic relief, and relative stiffness among the floor, coal pillar, and immediate roof will also contribute greatly to cutter roof development. It is not uncommon to observe cutter roof failures at a certain portion of a mine, but no trace of cutter roof formation can be found at other locations of the mine. The causes of cutter roof development are often different from mine to mine.

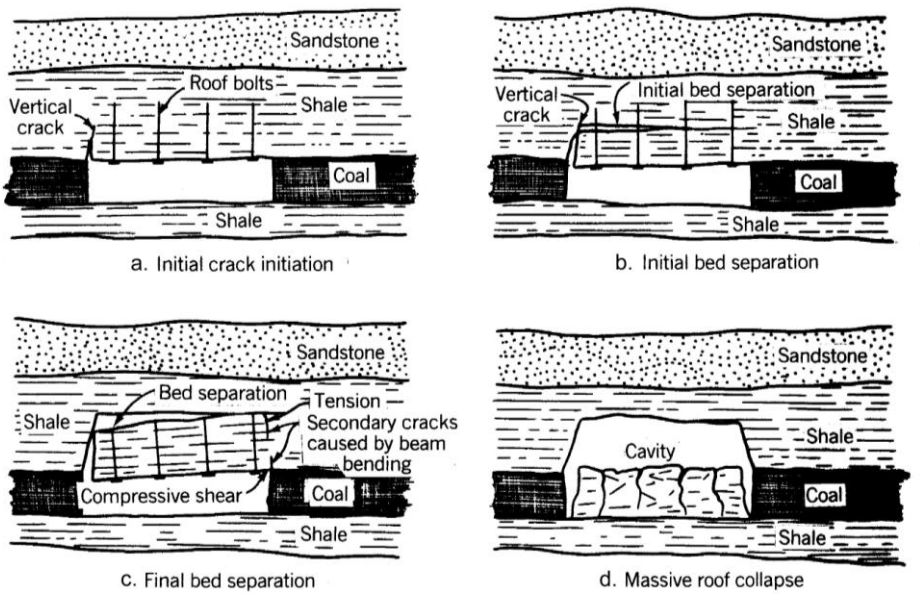

Fig. 10.3.2 propagation of cutter roof leading to roof fall (Kripakov, 1982)

10.3.2 Mechanisms of Cutters Formation

Figure 10.3.3 illustrates an example of a cutter formation (Peng, 2007). When exposed, the whole four layers were fractured at the intersection of roof and pillar rib. Due to free space below, the bottom layer of the immediate roof fell down and split into two pieces, 1a and 1b. Piece 1b dropped down more than, and moved toward, 1a. This resulted in a large gap between the first and second layers. The second layer is then free to drop and move laterally. This process repeats layer by layer upward. The layers in this case are rather uniform. In other cases, they may be much thinner or vary in thickness.

The mechanisms of cutter roof failures are divided into six categories based on studies by Hill (1988), Iannacchione et al., (1984), Kripakov (1982), and Su and Peng (1984 and 1985).

1. Higher Overburden Stress

The vertical stress in an underground coal mine increases with depth. A high vertical stress generally induces a high shear stress in the immediate roof at the entry corners and is the most influential parameter in cutter roof formation. Under a low horizontal stress environment, the high vertical stress controls the roof behavior at the entry corners, and fractures are more likely to propagate nearly vertically into the roof once they are initiated at the entry corners. In a high horizontal stress environment, the high vertical stress would still control the roof behavior at

the entry corners, although the roof behavior elsewhere in the immediate roof would be controlled by the differential stress and the absolute magnitude of the high horizontal stresses (Su and Peng, 1985; van der Merwe, 2000).

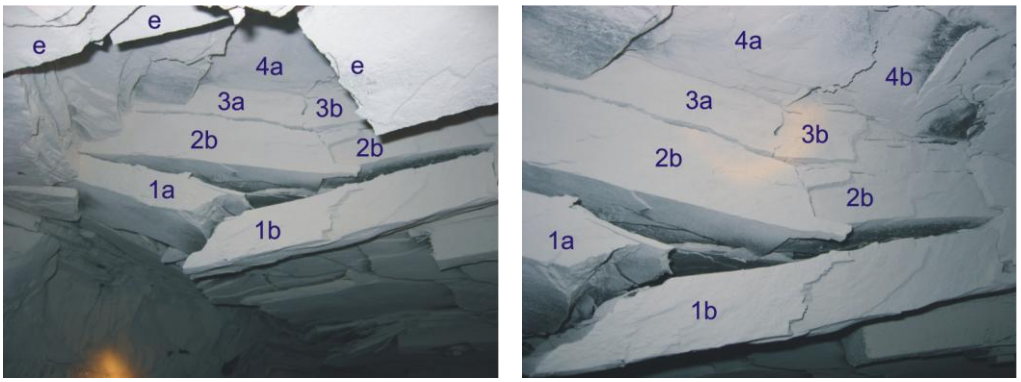

A B

Fig. 10.3.3 Development of a cutter. A and B are the same cutter in different views. Note that in B, rock piece "e" shown in A has been removed (Peng, 2007)

2. High Horizontal Stress

A high horizontal stress field with large differential stress (i.e., the difference in magnitude between maximum and minimum principal horizontal stresses are large) would contribute to the instability of the immediate roof. The differential stress would have a less pronounced effect on a softer immediate roof layer than a stiffer one. Under a given overburden stress, the differential stress would also have the least effect on the stability of the immediate roof layer at the entry corners. However, it would have the most effect on the stability of the stiffer layer at the midspan immediately overlying the immediate roof layer. As a result, cutter roof, if initiated at the entry corners, would most likely propagate at low angles into the roof under a high horizontal stress field with a large differential stress (Su and Peng, 1985).

The absolute magnitude of an excess horizontal stress field is sometimes more critical in contributing to roof stability than the differential stress, especially when both horizontal principal stresses are higher than the overburden stress. On the other hand, the direction of an excess horizontal stress field is also of great importance, as it dictates the location and nature of cutter roof occurrences. Figures 6.2.7 (p. 293) shows the preferred orientation of an entry/crosscut with respect to the maximum principal horizontal stress.

Finite element computer analyses (Aggson, 1979a; Kripakov, 1982) showed that the applied shear stress that causes cutter roofs is the difference between the major horizontal, σ_{h1}, and vertical, σ_v, in-situ stresses. When $\sigma_{h1} < \sigma_v$, the plane of maximum shear stress is inclined upward toward the pillar side, and a tensile fracture occurs in the roof at the entry center; when $\sigma_{h1} = \sigma_v$, the plane of maximum shear stress is vertical along the pillar rib; and when $\sigma_{h1} > \sigma_v$, the plane of maximum shear stress is inclined away from the pillar (i.e., inclined upward in the roof above the entry).

Computer modeling by Gadde and Peng (2005b) showed that the complex progressive failure mechanisms associated with cutter failures are extremely difficult to replicate in computer models. However, with a proper selection of the constitutive material behavior and

implementation of cutting sequence, it is possible to realistically reproduce cutter failure using continuum models.

For more discussion regarding cutter and high horizontal stress, refer to Section 6.3, (p. 303).

3. Relative Stiffness between Coal and its Immediate Roof

Variation of relative stiffness between coal and its immediate roof are fairly common from mine to mine or from one place to another in a given mine. The relative stiffness between coal pillars and the immediate roof rock has a pronounced effect on the development of cutter roof in the entries and crosscuts. As the first immediate roof layer becomes softer and the coal pillars become stiffer, cutter roof is more likely to occur near the rib-roof intersection when the mine is under thick overburden and in a low horizontal stress environment. On the other hand, under a high horizontal stress field with high differential stress, the horizontal stress concentration will arch deeper into the roof as the first immediate roof layer becomes softer. As a result, cutter roof is more likely to occur if the first immediate roof layer is stiffer.

The thickness of weak immediate roof overlying a coal bed is sometimes of great importance. Cutter roof is less likely to occur, and the roof tends to be more stable, if a thin immediate roof layer is overlain by a thick, competent sandstone layer. On the other hand, if the same immediate roof layer is overlain by a less competent rock layer with similar thickness, cutter roof is more likely to occur, and the roof tends to be less stable. In this respect, accurate determination and knowledge of the stratigraphic sequence is critical in designing roof support to prevent cutter formation.

4. Large Topographic Relief

Underground coal mine entries/crosscuts extend inevitably under varying overburden thicknesses, including large relief between mountain ridges and stream valleys at short distances. The stress fields under a steep or V-notch or a flat-bottom valley are quite different, as discussed in Section 6.4 (p. 305).

When the coal is relatively stiff with respect to the immediate roof, cutter roof is likely to occur under thick overburden (> 750 ft or 228.7 m) and a low horizontal stress environment. Under a high horizontal stress environment having large differential stress and the maximum principal horizontal stress perpendicular to the entries, cutter roof is more likely to occur in thinner overburden (< 500 ft or 154.2 m) than in thicker overburden. On the other hand, if coal is relatively soft with respect to the immediate roof, then with the same horizontal stress field, cutter roof failures plus midspan roof failures would occur in entries with overburden thinner than 500 ft (154.2 m). When the differential stress is small and the overburden thickness is around 470-570 ft (143.3-173.4 m), cutter roof may occur only at the upper right corners of the entries.

High vertical and horizontal stress concentrations exist at the upper right and lower left corners of the entries when the overburden is sloping from left to right. As a result, cutter roof would occur at the upper right corners of the entries, and floor cracks would occur at the lower left corners of the entries. Pillar spalling would also occur at the top section of the pillar to the right of an entry and at the bottom section of the pillar to the left of an entry. These types of spalling are frequently observed underground in entries adjacent to a longwall gob (Peng, 2007).

Moeb (as cited by Enever et al., 1978) studied the frequency of roof falls as related to their lateral distance from the center of valleys. He found that the risk of roof falls increases as the steepness of the valley wall increases and the depth of coal bed at the point of interest beneath the valley wall increases. Enever and Mckay (1980) also showed that when D/R is less than 0.5, a strong possibility of encountering adverse roof conditions exists. D is the depth at the point of interest and R is the maximum surface relief.

5. Geological Anomalies

Geological anomalies such as clastic dikes were found to have significant influence on cutter roof failures (Hill, 1988; Iannacchione et al., 1984). Clastic dikes, commonly known in mining terms as clay veins, range in thickness from 1 ft (0.3 m) of claystone matrix with fragments of shale and coal to as thin as a filmlike trace of calcite or clay. The dikes could extend as high as 30 ft (9.1 m) into the roof rock and would penetrate the coal bed at various angles. Few dikes would reach the floor rock. Fractures and slickensides in the roof were often associated with the presence of clastic dikes. Clastic dikes often form the boundary of roof falls resulting from cutter roof failures.

Hill and Bauer (1984) suggested that high frequency of clastic dikes in certain areas of a mine would increase the occurrence of cutter roof failures in these areas. Rock pressure monitoring near clastic dikes revealed that roof strata behave like cantilever beams. The cantilever beams would initiate cutter roof failure and develop along an entry or crosscut, often extending across several breaks.

10.3.3 Methods of Controlling Cutter Roofs

There are many methods that can be employed to control cutter roofs in an underground coal mine. The mine operators can vary such things as entry geometry, entry orientation, pillar geometry, and bolting patterns. However, selection of the best mining alternatives should be based on a complete understanding of cutter roof mechanisms. Possible mining alternatives for controlling cutter roofs are discussed in the following sections in terms of the mechanisms of cutter roof formation.

1. Adoption of a Larger Pillar While Keeping the Same Entry/Crosscut Widths

Large pillars will reduce the absolute stresses in the roof. This method can be applied to control cutter roof under high overburden stress or high horizontal stress. It is the easiest and the cheapest alternative available, although less coal recovery will be realized. The optimum pillar width depends on the overburden depth, horizontal stress, roof geology, and the material properties of the coal and roof rocks.

2. Adoption of Smaller Entry/Crosscut Widths While Keeping the Same Pillar Size

Smaller entries/crosscuts will also reduce the absolute stresses in the immediate roof. This alternative is most effective if the overburden stress is high. Theoretically, the opening should be as narrow as possible. However in practice, the opening should be at least 15-16 ft (4.8-4.9 m) wide for continuous miner operation.

3. Pillar Softening

FD Wang et al., (1974) proved that pillar softening for alleviating cutter roof problems is analytically sound and effective. It may also be useful for reducing roof failure and coal rib sloughing. This technique consists of drilling horizontal holes into the top of the coal pillar to

reduce the elastic modulus or the stiffness of the pillar. This change in the pillar produces a modified stress distribution in the roof near the pillar. This technique has been tested successfully underground (Maxwell et al., 1977).

Aggson (1978b) suggested that under hydrostatic stress, pillar softening could significantly reduce the maximum shear stress concentration at the entry corner. The effect of pillar softening in an area of high horizontal stress is rather small, however. On the other hand, where the horizontal stress is much less than the vertical stress, pillar softening can have negative results because it weakens the pillar's resistance. The tensile stress at mid-span of the roof would increase, although the shear and compressive stresses at the entry corners would decrease. As a result, tensile roof failure might occur at the center of the roof span. Therefore, the use of pillar softening should be attempted only after the stress conditions, mechanical properties of the roof, and failure mechanisms are fairly well understood. Pillar softening can be accomplished ahead of mining by drilling horizontal holes into the face that are angled out over the potential pillar. But, it is fairly difficult for this technique to be incorporated on-cycle into the daily production operations without causing production delays.

A 1-in. (25.4 mm) wide slot into the pillar along the roof line was found to be effective in reducing principal stresses at the corners of the roof and rib intersection. The reduction of stresses increases with the depth of the slot (Ahola et al., 1991). On the other hand, slotting at mid-height of the pillar was not effective.

4. Re-orientation of the Entries/Crosscuts

Re-orienting the entries to a direction parallel to the maximum horizontal stress would greatly improve roof conditions at the entry corners. However, this is done at the expense of roof conditions in the crosscuts that are perpendicular to the entries. This measure may be desirable, since crosscuts are normally used for storage and occasionally for ventilation. Other alternatives include: (1) orient the entry at 45^{o} to the maximum principal horizontal stress or (2) change the crosscut direction such that it is not perpendicular to the entry but oriented in the favorable directions with respect to the maximum principal horizontal stress.

For a more detailed discussion on the effect of entry/crosscut direction with respect to the direction of high horizontal stresses, refer to Sections 6.2 (p. 288) and 6.3 (p. 303).

5. Installation of Angled Bolts near the Ribs

Installation of large diameter angled roof bolts near the ribs will have little effect on the stress fields around the entry corners. However, if the angled bolts are installed with proper inclination so that they are more or less perpendicular to the fracture planes initiated at the corners, they will serve to increase the shear resistance along the fracture planes. In this way, installation of angled bolts can delay or prevent roof falls, resulting from the propagation of the fractures. Large diameter resin or cable bolts should be used. These bolts should be sufficiently long to reach deep into the roof above the pillar. The deeper anchorage horizon would retard cutter roof failures since the fracture would normally propagate across the entry at or slightly above the anchorage horizon of shorter roof bolts. This method of roof support is most effective if the fracture plane deviates considerably from the vertical.

Khair (1992) studied methods for alleviating problems associated with cutter roofs in a coal mine in Pennsylvania where the immediate roof was broken up under extremely high horizontal stresses. He found that yield pillars were not effective in dealing with cutter roofs and that proper design and implementation of roof reinforcement system (i.e., longer and larger

diameter bolts in the proper pattern) can be used to stabilize the roof and eliminated roof caving during entry development and retreat longwall mining, even though cutters persisted throughout the mining operations.

6. Installation of Trusses and Cribbings

Trusses and cribbings were found to be effective in stabilizing clastic dikes and inhibiting the development of cutter roof failure when employed immediately after mining. Cribbing is labor intensive and time-consuming, although it is very effective in stabilizing the roof. Installation of roof trusses or cable trusses normally creates a compressive force vertically downward near the rib edge of the pillar. This compressive force would increase the rock strength at the rib/roof intersection if in-situ high horizontal stress is the main cause of cutter roof failure, thus making the roof or cable trusses more effective in controlling cutter roof.

Staggering crosscuts would prevent the extension of the cutter and deter the occurrence of large falls extending over several breaks. Similarly, stepped ribs larger than 1 ft (0.3 m) deep that result from uneven cutting between consecutive cuts of the continuous miner have also been found to stop the extension of a cutter.

10.4 RIB FALLS

10.4.1 Definition and Characteristics

Rib falls, rib rolls or **rib sloughing** is the dropping of material from the pillar ribs. The material is mainly coal, but may involve rocks if the mining height includes roof or floor rock or partings or a combination of them. Strictly speaking, rib rolls are the initial stage of pillar failure, which may or may not progress further. Sometimes they are associated with the early stages of the failure of insufficiently sized pillars or are the effect of depth (Bauer et al., 1999). Under the prevailing mining depth conditions in U.S. underground coal mines, rib rolls occur and may become a safety hazard when the pillar height exceeds 8-10 ft (2.4-4.05 m).

Rib falls range from minor to as large as 45 ft (13.7 m) high by 60 ft (18.3 m) long (Robinson et al., 2007). From a safety point of view, the size of spalling, the manner in which it occurs, and the time of occurrence are critical factors. Obviously, failure of a large block is dangerous, while continuous falling of small pieces also has negative effects. They can create large overhangs that may fall in large blocks, and/or increase the entry width and decrease pillar width, reducing pillar strength (Vervoort, 1992).

According to Bauer et al., (1999), the rib and roof skin failure injury rate increased with seam height, peaking at 8 ft (2.4 m).

For more discussion regarding rib sloughing, refer to Section 5.6.1 (p. 269).

10.4.2 Types of Rib Falls

Rib rolls occur in several forms (Peng, 1986, Maleki, 1992; Robinson et al., 2007). They may be stress-induced or geologically-controlled. Stress-controlled rib rolls occurred in slender pillars under high overburden depth. Sloughing may take the form of vertical slices peeling off the sides of the pillars (Fig. 10.4.1B). Geologically controlled rib spalling includes cleats and joints (Seedsman, 2006). Rib rolls may be induced by soft partings that were squeezed and expanded laterally (Fig. 10.4.1A).

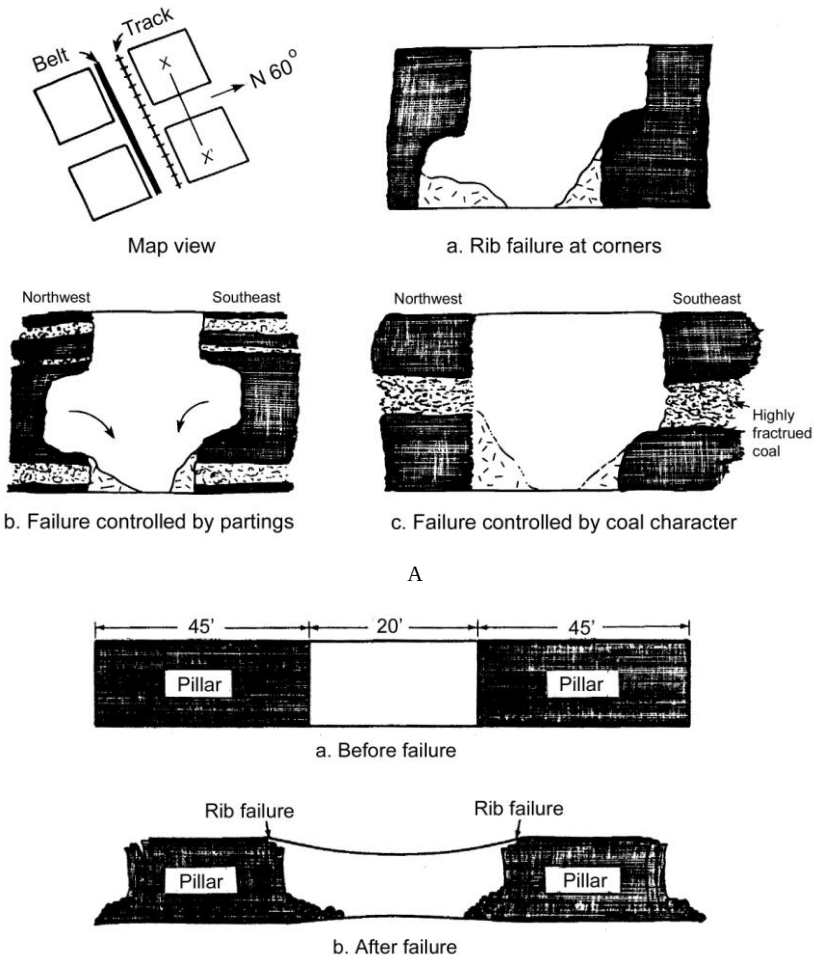

Fig. 10.4.1 Examples of rib sloughing (Peng, 1986)

Under normal conditions in which the roof and floor rocks are stronger than the coal pillar ribs, the ribs may fail in four ways: compression shear sliding, gravity sliding, vertical slabbing, and hour-glassing (Yang, 2005).

1. Compression-Shear Sliding

When the ribs are intact with residual strength and subjected to high abutment stress from the roof, failure of ribs will be from compression-shear sliding (Fig.10.4.2).

According to the Mohr-Coulomb theory, the angle between the compression-shear sliding face and the rib surface is:

$$\beta = 45° - \frac{\phi}{2} \tag{10.4.1}$$

where ϕ is the internal angle of friction.

The maximum depth of rib sloughing is:

$$\Delta d = H \tan(45° - \frac{\phi}{2}) \tag{10.4.2}$$

where H is entry height.

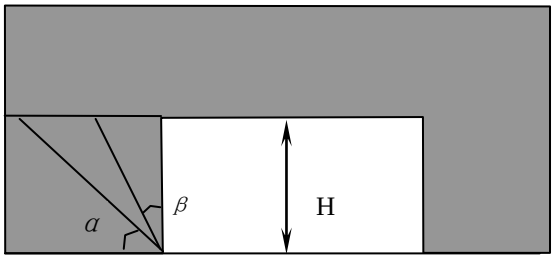

Fig.10.4.2 Rib Falls - compression-shear and gravity sliding (Yang, 2005)

2. Gravity Sliding

If the ribs are in a completely broken state with no residual strength left and subjected to self-weight, failure of ribs will be in the gravity sliding mode (Fig.10.4.2).

The angle between the gravity sliding face and the rib surface is:

$$\alpha = \phi \tag{10.4.3}$$

where ϕ is the internal angle of friction.

The maximum depth of rib sloughing is:

$$\Delta d = H \cot \phi \tag{10.4.4}$$

3. Vertical Slabbing/Buckling

If the ribs are not broken completely, and there are well-developed cracks perpendicular to the bedding after being subjected to abutment pressures, the ribs will expand laterally and fail in a vertical slab by buckling (Colwell and Mark, 2005; Hebblewhite, 2006) (Fig.10.4.3).

The maximum depth of rib sloughing is affected mainly by the entry height, the strength of ribs, the distribution of abutment pressure, and crack distribution.

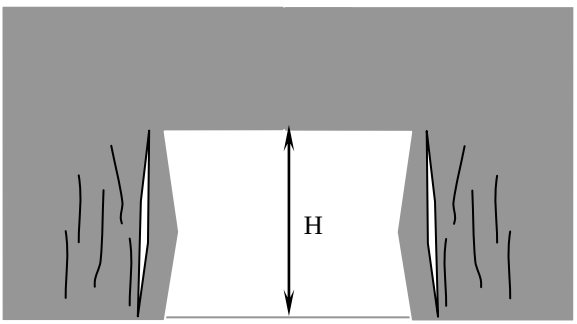

Fig.10.4.3 Rib fall - vertical slabbing (Yang, 2005)

4. Hour-Glassing

If the ribs are broken completely and subjected to abutment pressure, the ribs will expand outward, and if the blocks are sufficiently large, the ribs will fail to assume an hour-glass shape (Fig.10.4.4).

The maximum depth of rib sloughing is:

$$\Delta d = \frac{H}{2f} \tag{10.4.5}$$

where f is the Protodyakonov scale of hardness and equal to

$$f = \frac{\text{UCS}}{10} \tag{10.4.6}$$

where UCS is the uniaxial compressive strength in MPa.

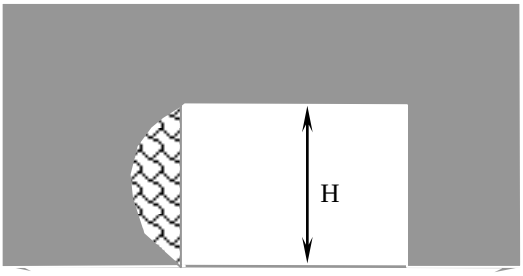

Fig. 10.4.4. Rif falls – hour-glassing (Yang, 2005)

Rib falls have also been attributed to horizontal stress (Robinson et al., 2007; Jeremic, 1981). When roadways are perpendicular to lateral tectonic stress, rib spalling up to 4 in. (100 mm) occurs during development and expands to 5 ft (1.5 m) one year after development; When roadways are parallel to the lateral tectonic stress, pillar spalling occurs around mid-height, forming an hour-glass shape, and the depth of spalling is only half of that when roadways are perpendicular to lateral stress. When roadways are oblique to lateral tectonic stress, ribs are stable except at intersections. The diagonal corners along the direction of lateral tectonic stress are sloughing severely, up to 10 ft (3 m) a year after development, while the diagonal corners perpendicular to lateral stress are stable (Jeremic, 1981).

10.4.3 Rib Fall Control

Rib bolts, similar to roof bolts are the major support system for rib control. The key factors in the control or prevention of skin failures due to rib rolls or shallow roof falls between bolts or rows of bolts are coverage and large deformation.

Coal is a soft material with many defects and thus deforms with time. It does not provide good anchorage, especially when ribs yield (Larson and Dunford, 1996) and cannot be constrained by a low density of rib bolts. Consequently the same roof bolting principles developed for roof support must be modified when applied to rib support. Underground monitoring of rib bolt behavior showed that the effects of the conventional fully grouted bolts are localized, because the soft and weak material is unable to transfer the load beyond a small radius around the bolt (Hebblewhite et al., 1998). In addition, lateral displacement of pillar ribs

in greater mining height and thick cover, for which rib supports are required, is also great, such that most high-strength stiff bolts designed for roof support are not desirable for rib support.

Against this background, many different types of rib bolts have been developed (Howarth and Renwick, 1992; Skybey, 1995). In the U.S., rib support generally consists of fully grouted resin bolts, 4-5 ft (1.2-1.5 m) long, either one or two rows at 4 ft (1.2 m) intervals. If it is one row, the bolts are usually installed at mid-height; If it is two rows, one is at mid-height and the other is at the top one-third of the height. For area coverage, a wood plank is inserted between the bearing plate and rib surface. At the minimum, the coverage should include the use of regular roof mat and in severe cases, "Monster" mat with a row of bolts (Bauer et al., 1999). Alternatively, "pizza pans," in conjunction with the regular bearing plate should be used. A **pizza pan** is a square, non-graded steel plate 17 in. (431.8 mm) wide with strength ranging from 550 to 1,375 lbs. (2.45-6.12 KN) (Tadolini and Dolinar, 2001).

In deep mines, the stiff resin bolts may be broken due to increased rib dilation or large rib deformation during longwall retreat. For this reason, Martin et al., (1988) developed a yieldable, tubal device to be used in conjunction with regular roof bolts. It is simply a 14-gage tube inserted over the bolt and held in place between the bolt head and bearing plate (Fig. 10.4.5).

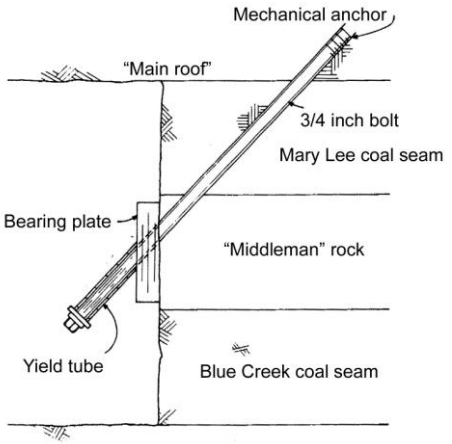

Fig. 10.4.5 Yieldable rib bolt (Martin et al., 1988)

For coverage of roof and rib against skin failures, synthetic materials such Tensar (Fig. 10.4.6) are used to cover the roof and ribs either fully or partially. Sometimes wire screen with or without shotcrete or polymer membrane liners (Laurence et al., 2000) is used.

10.5 SHALE AND ITS ROLE ON MINE ROOF STABILITY

10.5.1 Introduction

Shale is the most abundant rock material associated with coal mines and forms the great majority of roofs and floors in underground coal mines. Other than fine-grained, the term "shale" is ambiguous. Many descriptive adjectives have been used by geologists to describe shale found in the loggings of exploration boreholes. Those descriptions in most cases add confusion for practitioners; much less contribute to the understanding of the rock property as ground control materials. Experience has shown that the quality of shale as a coal mine

structural element varies considerably. Some shale serve as a good roof, while others are very poor roofs (Gurgenli and Peng, 2006). In fact, most roof falls and unstable roofs occur in shales. How to determine the quality of shale as a coal mine ground control structural element? What makes a good shale roof and vice versa? These questions must be answered and understood, due to the abundance of shale in coal mine roofs and floors.

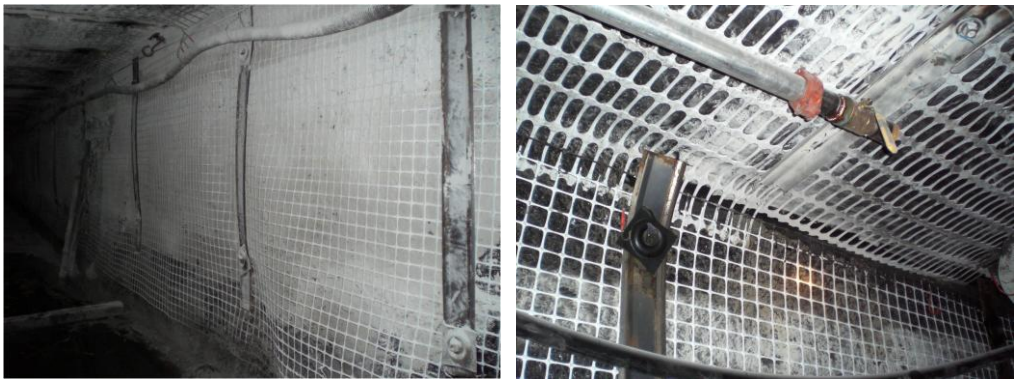

Fig. 10.4.6 Rib (left), and rib and roof (right) control with tensar screens

10.5.2 Composition

Shale is fined-grained, highly-compacted and contains various amounts of clay. It exhibits fissility or splitting along closely spaced, nearly parallel surfaces, or laminations. The major components of coal mine shales are clay, quartz, mica, and other trace minerals as shown in Table 10.5.1 (Holland, 1958a). The major clay minerals are illite, kaolinite, and chlorite, while montmorillonite rarely exists. Clay particles are oriented in various degrees; the higher the preferred orientation, the more absorbent and the lower the strengths are (Aughenbaugh and Bruzewski, 1976; Bodus, 1989).

Table 10.5.1 Minerals in coal mine roof shales (Holland, 1958a)

Mineral	Percentage	Mineral	Percentage
Clay Illite Kaolinite Chlorite Montmorillonite	5 - 75 3 - 60 2 - 30 0 – 15 0 - 10	Coal [1]	3 - 50
		Chlorite	1 - 20
		Unconfined water	1 - ?
		Iron sulfide	0.1 – 12
		Feldspar	0 - 45
Mica	5 – 60	Soluble salts	0.05- 3
Quartz	5 - 35	Siderite	0 – 12
		Calcite	0 - 15

[1] Including other organic matters

10.5.3 Weathering

1. Mechanisms of Weathering

Weathering refers to those changes in shale roof as a result of being in contact with the mine atmosphere or, in some cases, to changes caused by the combined action of groundwater and

the mine atmosphere. Shale changes its properties due to changes in moisture, temperature, and the presence of oxygen and carbon dioxide. The intensity and severity of changes in shale depend on the type and amount of minerals present. Thus, a shale when first under- or over-mined and exposed to atmosphere conditions may have properties corresponding to a rock, but its properties may change with time to those equivalent to soil. The following properties of minerals are key to shale weathering.

A. Ion and water exchanges

Ions, both anions and cations, can be absorbed and exchanged in a water solution or sometimes in a non-aqueous environment. Clay minerals with ion exchange capacity in descending order are montmorillonite, illite, chlorite, and kaolinite.

All shales contain water. In terms of weathering, only the water that exchanges with the mine atmosphere and that changes in relative humidity at the mine's temperature will be considered here. Water controls the effects of plasticity, expansion or contraction, and slaking of roof shales.

B. Plasticity

The plasticity of clay minerals depends on the type, particle size, geometric features of minerals, and types of cations present. Clay can absorb a lot of water before plasticity sets in. Thereafter, any slight increase in water causes an abrupt change in plasticity to occur. Consequently the plasticity effects may develop quickly in shale roof once in contact with mine air.

C. Expansion and contraction

Expansion and contraction of roof shales are believed to be the most destructive weathering effects. During expansion, a relaxation of effective compressive stress enlarges the capillary films and osmotic imbition of water by expanding lattice clays. Expansion perpendicular to the bedding plane is five times that parallel to the bedding plane. During contraction, the two mechanisms act in reverse.

Singh and Cummings (1983) tested the expansion of claystone and gray and black shales. They found that expansion perpendicular to bedding planes are 7 and 2 % for claystone and shales, respectively; that compared to the perpendicular direction, expansion along the bedding plane direction is insignificant; and that shales containing clay expand more than those with little clay. Huang et al., (1995) found that the major factors controlling expansion of shale are air humidity tempering, and the moisture activity index (see p. 491). Shales exposed initially to air with low relative humidity (0-44 %) have much less marked changes and exhibit very similar expansion responses (Huang et al., 1986b). But at higher relative humidity (44-100 %), the expansion accelerates with increasing relative humidity (Huang et al., 1986a; Van Eeckhout and Peng, 1975).

D. Slaking

During drying, the shales shrink creating cracks. The water evaporates and is replaced by air. As water is reabsorbed, the air is entrapped and compressed in capillary openings, causing tensile stresses in shale. Simultaneously, clay minerals expand once water is absorbed, setting up differential stresses in shale. The stresses caused by the entrapped air and expanding clay minerals act to cause the clay to slake.

E. Chemical alteration

Shales contain various amounts of iron sulfides, F_eS_2, that oxidize to form F_eSO_4 and H_2SO_4 in the presence of moisture and oxygen. F_eSO_4 occupies several times the volume of the original F_eS_2, causing high local stresses. H_2SO_4 may reacts with other minerals, weakening the shale further and creating more high local stresses. Siderite and ferrous iron in illite, when oxidized, shrink in volume up to 27.5%. In summary, oxidation in general decreases the strength of shale and causes soluble salts to effloresce.

F. Clay minerals

The strength of shales is, in part, a function of the preferred orientation of clay minerals within them. Measurement of fabric changes between dry and wet condition is helpful in understanding roof shale failure. Studies of shales in the roof of the Herrin #6 seam in the Illinois coal field by Bodus (1989) showed that under air-dried conditions, Anna shale is the most stable, followed by energy and Lawson shales; and under mine conditions, energy shale is the most stable followed by Anna and Lawson shales. When underground roof failures involve shales, unique physical changes are noted. Those changes are also found in the laboratory, including (1) increased hydration around the perimeter of iron concretions in energy shale, (2) radial extension cracks in Anna shale, and (3) extreme slaking of Lawson shale.

Kaolinite and montmorillonite react with water and cause a substantial deterioration in the shale (Zhang et al., 2004). Figure 10.5.1 shows that shale strength is reduced with increasing content of montmorillonite when wet (Matsui et al., 1996). Note that S_{cw} is shale strength with a certain content of montorillonite, W_{mo}, and S_{cd} is shale strength without montorillonite.

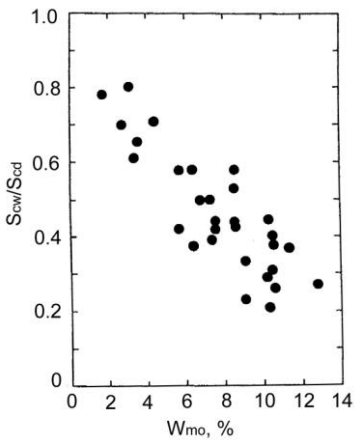

Fig. 10.5.1 Shale strength decreases with increasing content of montmorillonite (Matsui et al., 1996)

2. Stress Developed by Water Adsorption

Figure 10.5.2 shows a test simulating a more realistic underground mine roof condition in which only the exposed roof rock surfaces are exposed and in contact with moisture carried by the moving ventilation air. The test is set up for measuring stresses generated by water absorption in a cylindrical shale specimen (Chenevert, 1970). A small hole was drilled axially through the specimen encased in an impermeable jacket. Strain gages were attached and the hole was filled

with water at 100 psi (0.69 MPA) and kept at 75°F (23.9°C) throughout the test. As the specimen absorbed water, hydraulic pressure was applied on the outside of the cylinder in order to keep zero strain on the wellbore surface. In an hour, the shale developed stress of 1,000 psi (6.9 MPa); 5,200 psi (35.86 MPa) after 24 hours; and after 39 hours, the stress changed abruptly indicating specimen failure. Inspection of the wellbore after test termination showed that the wellbore was enlarged about 2.5 times and chips were produced through spalling.

The stress, σ_w due to moisture absorption, developed in shale can be predicted by

$$\sigma_w = \frac{RT}{V} \ell n \frac{p}{p_o} \tag{10.5.1}$$

where R = 0.083 liter atm/mol °K, is a gas constant, T is absolute temperature, °K, V is partial molar volume of pure water, p and p_o are aqueous vapor pressures of shale and water, respectively, in atm, p/p_o = relative humidity.

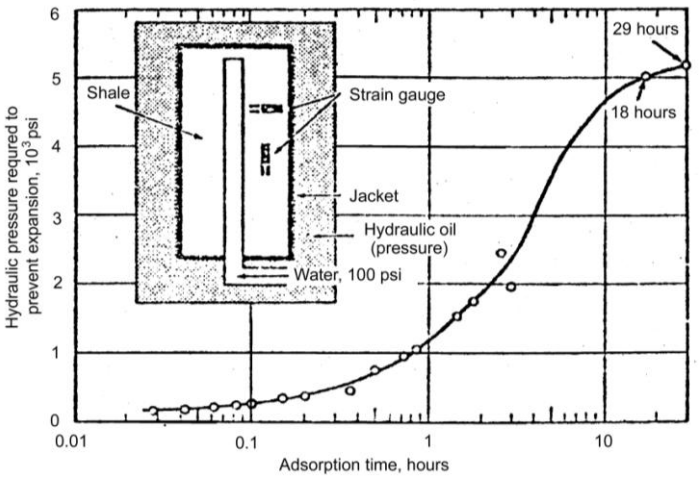

Fig. 10.5.2 Hydraulic stress developed by water adsorption (Chenevert, 1970)

Aughenbaugh and Bruzewski (1976) and Huang et al., (1986a) measured the swelling pressure by injecting water to the circumference of a cylindrical specimen, and keeping the axial pressure constant. The maximum pressure measured was 14,000 psi (96.5 MPa). Shales with even trace amounts of clay minerals can generate a fairly large expansion force. Also shales without smectite minerals can have significant swelling, suggesting that clay content and type of clay minerals are not the only factors influencing shale expansion. Other factors such as particle arrangement and pressure release also play a role in shale expansion (Huang et al., 1986b).

Therefore, when clay absorbs moisture, the stresses generated can easily crush the surrounding rocks.

3. Laboratory Tests for Determining Weatherability of Shales

There are several methods available for determining the weatherability of shales: slake durability index, moisture activity index, weatherability index, water content, swelling strain (Gurgenli and Peng, 2006), and water sensitivity (Hasenfus and Su, 2005) tests. A description of those methods follows.

A. Slake durability index test

The slake durability test uses a cylindrical 0.08 in. (2 mm) sieve screen, into which a rock sample is placed. The screen is lowered into a bath of water and is rotated on its axis for a period of 10 minutes. Portions of rock that deteriorate in the presence of water, or due to the mechanical action of the rotating screen or both, drop through the screen into the water bath. After two cycles, the weight percentage of the original sample that is retained on the screen is the slake durability index.

The water sensitivity test (Hasenfus and Su, 2005) is a modified slake durability test. The general procedure is as follows:

(1) Core or grab samples are wrapped in plastic or equivalent to prevent moisture loss and degradation.
(2) Samples are selected, inventoried, and logged including lithology and characteristics. Core samples, ranging from 3 to 6 in. (76.2-152 mm), are segregated as best as possible by lithologic boundaries. Lithologic units less than 3 in. (76.2 mm) are combined with adjacent units. Grab samples total at least 0.66 lb (300 grams) (ambient weight). Individual grab pieces are at least 0.33 lb (150 grams) in weight with a minimum least dimension approximating 1.5 in. (38 mm).
(3) Samples are weighed for ambient weight (W_a) to at least 0.1 gram and placed in a drying oven set to between 212°F (100 °C) and 221°F (105 °C) for a period of 24 to 48 hours.
(4) After drying, samples are cooled for about 1 hour and weighed for dry weight (W_d). Samples are then immersed completely in a container filled with tap water for a period of 24 to 48 hours.
(5) Samples are wet-sieved (under tap) via a stacked pair of sieves; 0.75 in. (19 mm) mesh over 0.08 in. (2 mm) mesh screens. After sieving, the retained and separated +0.75 in. (19 mm) and +0.08 in. (2 mm) sieve portions are then re-dried at 212°F (100 °C) to 221°F (105 °C) for a period of 24 to 48 hours.
(6) After drying, samples are cooled for about 1 hour, and the individual +0.75 in. (19 mm) and +0.08 in. (2 mm) portions are weighed (W_{19} and W_2 weights, respectively).

The resulting water sensitivity indices are calculated as:

$$WS_{19} = 100\ (W_d - W_{19}) / W_d \qquad \text{(19 mm index)}$$

$$WS_2 = 100\ [(W_d - (W_{19} + W_2)] / W_d \qquad \text{(2 mm index)}$$

Water sensitivity indices generally correlate with the clay mineralogy and relative strength of various rock types. Clay-rich rocks have the highest water sensitivity indices (both WS_{19} and WS_2), being greater than 56%, while sand- and lime-rich rocks have WS_{19} < 30-35%. Hasenfus and Su (2005) found the water sensitivity indices to be more applicable to evaluating floor rock degradation than the standard slake durability index. The 0.75 in. (19 mm) screen size provides greater discrimination, while the 0.08 in. (2 mm) screen provides qualitative information about clay content.

B. Moisture activity index test

The moisture activity index or relative humidity test was proposed by Aughenbaugh (1981) to explain shale durability with respect to humidity conditions. A humidity chamber that can control relative humidity is used. The testing procedures are:

(1) Oven dry the samples for 16 hours at 230° ± 9°F(110° ± 5°C).

(2) Weigh and place the specimens inside a humidity chamber at a relative humidity (RH) ranging from 0 % to 100 %.
(3) Weigh the specimens each day, and if no more change is observed in the weight of the specimen, increase the relative humidity to the next higher level and repeat this step to the end of 100 % RH.
(4) Calculate the percent weight change (or water content) at the specific relative humidity as follows:

$$\text{Weight change (\%)} = \frac{\text{Final specimen weight - Dry specimen weight}}{\text{Dry specimen weight}} \text{ x } 100$$

(5) Calculate the moisture activity index (I_{RH}) as follows:

I_{RH} = % weight change @100% RH - % weight change @ 20% RH

Based on the test results, shales are classified into four categories:

a. When $1 > I_{RH}$, it is stable
b. When $1 < I_{RH} < 4$, it is mildly susceptible
c. When $4 < I_{RH} < 7$, it is moisture sensitive
d. When $7 \leq I_{RH,}$ it is non-durable

C. Weatherability index test

The weatherability test of rocks in underground coal mines was introduced by Unrug (1997). It is designed to simulate weathering cycles in mines at accelerated rates. The test procedures are (Fig. 10.5.3):

(1) Oven dry the specimens for 16 hours at $230^o \pm 9^oF$ ($110^o \pm 5^oC$).
(2) Weigh and put the specimens inside a tank and take photographs.
(3) Soak the specimens with water for 1 hour (wet cycle).
(4) Dry the specimens for 6 hours by running the installed fan (dry cycle).
(5) Repeat steps 3 and 4 and check the specimens for three cycles.
(6) Terminate the test and take photographs.
(7) Pick up the largest elements of the specimens surviving the test and dry them in the oven for 16 hours at $230^o \pm 9^oF$ ($110^o \pm 5^oC$).
(8) Calculate the weatherability index, WAI (%), as:

$$WAI = \frac{\text{Weight}_{\text{initial}} - \text{Weight}_{\text{remaining}}}{\text{Weight}_{\text{initial}}} \text{ x } 100$$

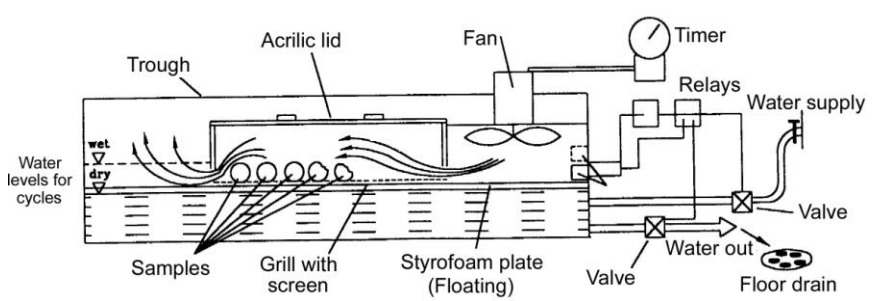

Fig. 10.5.3 Schematic of the weatherability test apparatus (Unrug, 1997)

In a study of roof rocks from 14 coal mines in various U. S. coalfields, Molinda et al., (2006) found that the WAI ranges from completely non-reactive (WAI $\approx$ 0) to those that are disintegrated into mud within 60 seconds (WAI = 100). For those six mines with WAI $\geq$ 50 %, all had significant roof problems related to scaling and slaking.

D. Swelling strain test

The swelling strain test was described by Van Eeckhout and Peng (1975) as:

(1) Place the specimens inside a humidity chamber such that laminations are in the horizontal direction.
(2) Employ strain gages or dial indicators to measure strains either in vertical or lateral directions.
(3) Maintain the desired humidity levels, e.g., 20%, 50%, 80%, and 100% RH.
(4) Record displacements each day until no more change is observed at each RH level.
(5) Increase the humidity to the next higher level and continue recording.
(6) Stop at the end of 100% RH and calculate the unconfined swelling strain, ε_h (%), as: $\varepsilon_h = d/L$ x 100, where subscript h is a direction relative to the bedding, d is the maximum swelling displacement (in.), and L is the initial length in the direction h (in.).

The swelling strain measured by Gurgenli and Peng (2006) ranged from 1.07 to 4.30 %. Shales that attained 4.3% strain deteriorate quickly after mining.

E. Summary

In a study of coal mine roof shale in the central coalfield, Gurgenli and Peng (2006) found that the moisture activity and weatherability indices are representative of shale behavior. This conclusion conforms to those by Aughenbaugh (1981) and Molinda et al., (2006) in that the weatherability index is a good indicator for shale behavior in underground coal mines.

The above-mentioned weather-sensitive properties can be used to classify shales into various categories in terms of their response to weathering and thus entry stability (Sickler, 1986).

4. Methods of Controlling Weatherability of Shales Underground

Many shale roofs are highly sensitive to moisture and weathering, i.e., wet and dry cycling, and exhibit significant time-dependent behavior. This type of shale is prone to roof falls and difficult to control with artificial supports (Fig. 10.5.4), if they are sufficiently thick (Zhang et al., 2004). Several methods are available to control its adverse effects, including air tempering, air conditionings, leaving the top coal unmined, and spray coating.

A. Air Tempering/air conditioning

Since the wet and dry cycles of ventilation air in summer and winter cause cracking in underground roof shales, the best way to control shale deterioration with time is to maintain constant humidity or moisture in the air. This can be done either through **air tempering** or **air conditioning** or both.

(1) Air tempering

In this method a tempering chamber is used to bring the fresh air entering a mine into equilibrium with the mine conditions through changing the temperature and humidity levels.

The summer air is warmer and has more moisture than the mine air, resulting in cooling and condensing of the excess moisture. In winter, the opposite is true. The amount of water condensed upon coursing through the mine can be substantial. For example, consider 90°F (32.2°C) intake air at 90 % relative humidity. After passing through the air tempering chamber, the air will be at 70°F (21.1°C) and 60 % relative humidity (Haynes, 1975). The moisture loss is,

Moisture level @ 90°F (32.2°C), 90% RH: 14.81 x (90/7008) = 0.1902 lb/ft^3
Moisture Level @ 70°F (21.1°C), 60% RH: 7.99 x (60/7008) = 0.0684 lb/ft^3
The net loss = 0.1902-0.0684 = 0.1218 lb/ft^3 of dry air.

If the mine is ventilated with 200,000 cfm, then the total moisture loss is

0.1218 lb/ft^3 x 200,000 ft^3/min = 24,360 lbs/min = 12.18 tons/min.

The fresh air, upon entering a tempering panel, is split from a single entry into eight or more entries. This dispersion of the air reduces its velocity and puts it in contact with a greater amount of mine surface, resulting in a more rapid conditioning of the air in terms of temperature and humidity.

By pre-conditioning the intake air before it reaches the working or transportation areas, the adverse effects of seasonal weather changes are restricted to the intake entries/crosscuts leading to the air tempering panels and in the area inside the tempering panels.

Fig. 10.5.4 An example of a roof fall (two scenes) due to weathering of weak roof (Peng, 2007)

a. Case 1

Aughenbaugh and Bruzewski (1973) found that there was a five fold increase in the humidity level by weight from winter to summer; that the severe surface temperature and humidity fluctuations are dampened significantly at the shaft bottom; and that the inby distance required for the air to stabilize at near constant humidity and temperature depends mostly on the rate of air flow. The larger the air flow, the longer the inby distance required to stabilize the temperature and relative humidity. When the air flow delivered by the main fan was 150,000 cfm (ft^3/min) (70.8 m^3/sec), the inby distance required was 1,500 ft (457.3 m). When the air flow was increased to 200,000 cfm (94.4 m^3/sec), the inby distance required was increased to 4,000 ft (1,219.5 m).

Figure 10.5.5 shows the schematics of a ventilation plan of a coal mine in the central coalfield, including location of weather/deflection station, where air tempering was practiced. The weather/deflection stations continuously measured the air temperature and relative

humidity as well as roof convergence for 2.5 years. Stations 1 and 2 were installed 420 ft (128 m) and 3,700 ft (1,128 m) inby the intake air shaft bottom, respectively. Stations 3 and 4 were installed in a panel, one on the intake side and the other on the exhaust side. When stations 3 and 4 were initially installed, the panel was actively being mined. As soon as mining was completed, the panel was converted into a tempering chamber for the intake air before it reached the working faces. Thus, stations 3 and 4 monitored the intake and exhaust conditions during panel development and then used as a tempering chamber for the mine's atmosphere.

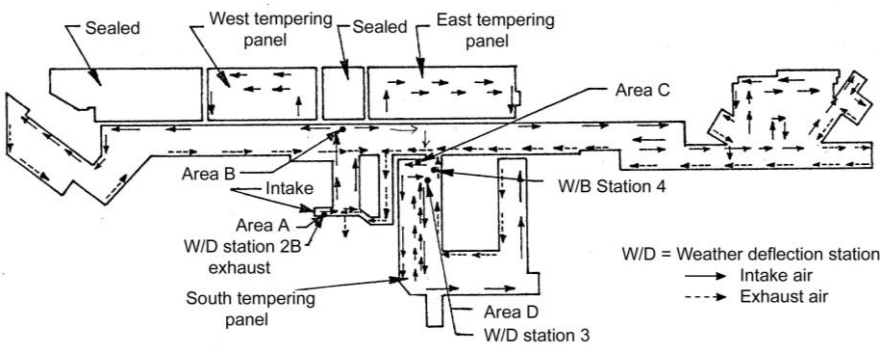

Fig. 10.5.5 Mine layout showing mine ventilation plan and location of air tempering section (Aughenbaugh and Bruzewski, 1973)

For station 1 (Fig. 10.5.6A), the temperature and humidity distinctly reflected the outside seasonal weather changes. The roof at station 1 was stable, converging nearly 0.2 in. (5.1 mm) in 2.5 years. The roof convergence curve was steeper in the spring and summer than in the fall and winter.

For station 3 (Fig. 10.5.6B), the temperature was essentially constant. The absolute humidity (i.e., the weight of water vapor contained per unit weight of dry air) still reflected seasonal trends, though the variations were much smaller. The roof converged slowly except for two periods and then totally stabilized. The roof converged a total of 0.068 in. (1.73 mm).

For station 4 (Fig. 10.5.6C), the temperature and humidity show distinct leveling off after completion of panel mining without any discernable seasonable changes. The absolute humidity stabilized at 0.38 lb/in^3 (10.5 gm/cc). The roof convergence stabilized at 0.02 in. (0.51 mm) during the 1.5 years monitoring period.

Therefore, the roof rock dries continuously in the winter, and it absorbs moisture in the summer. The air leaving the panel has a higher absolute humidity than that entering, regardless of the season.

b. Case 2

Cummings et al., (1981) evaluated the effectiveness and feasibility of using air tempering entries in an eastern coal mine to reduce or stabilize humidity levels. The air tempering entries were located at the bottom of the mine shaft. They found that temperature equilibrium was largely complete within 5 minutes residence time, while humidity needed about 30 minutes to stabilize. Both temperature and humidity (air moisture) dropped quickly as the fresh air entered the air tempering entries. The rate of air moisture decrease slowed down until after about 20 minutes air resident time. Air velocity in the air tempering entries should be less than 300 ft/min (1.52 m/sec).

In mid-summer, the air tempering entries were foggy and roof surfaces were wet. Small pieces of roof fall continued, being more severe near the air inlet and less near the outlet. In winter, the roof was dry and roof falls stopped. The mains' air tempering entries suffered little deterioration throughout the year. However, the life span of the air tempering entries could not be evaluated.

The zones and times of maximum roof convergence correlated with the changing positions of mine air equilibrium zones.

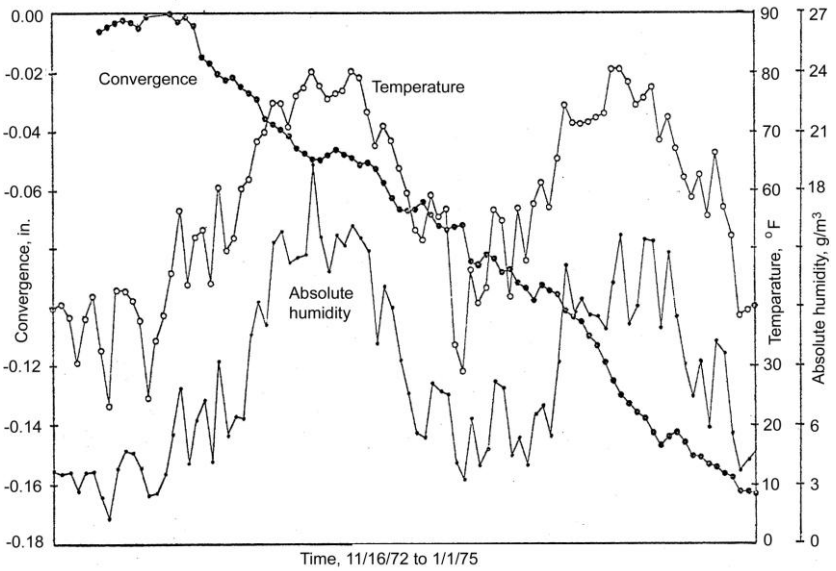

Fig. 10.5.6A Weather/roof convergence history for station 1 (Aughenbaugh and Bruzewski, 1976)

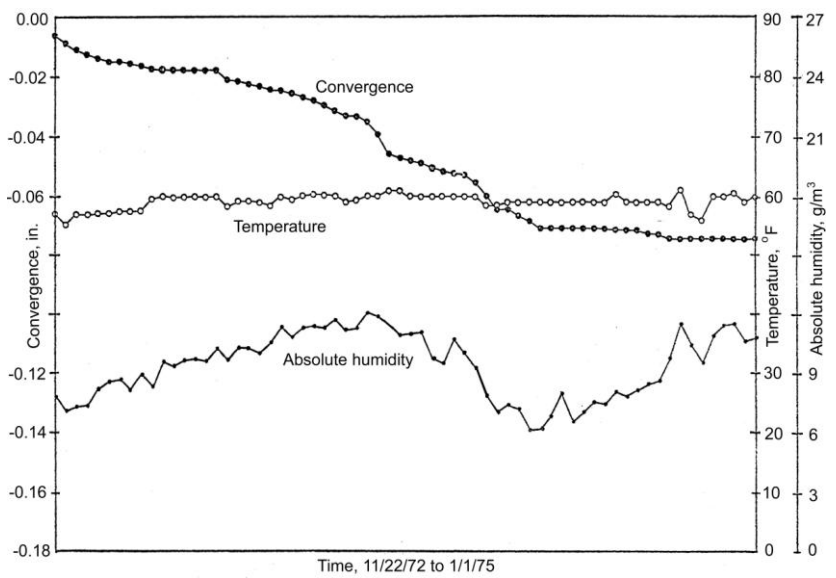

Fig. 10.5.6B Weather/Roof convergence history for station 3 (Aughenbaugh and Bruzewski, 1976)

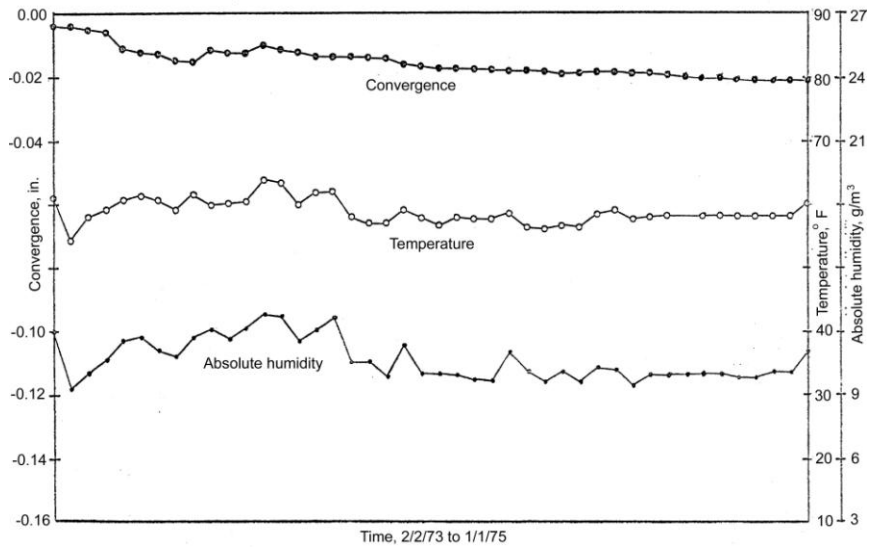

Fig. 10.5.6C Weather/roof convergence history for station 4 (Aughenbaugh and Bruzewski, 1976)

(2) Air conditioning

Another method of supplying ventilation air with constant moisture throughout the year is to apply air conditioning in the summer months when the air is humid. Zhang et al., (2004) reported a case demonstrating the beneficial effects of air conditioning. In a coal mine in the central coalfield, air conditioning was not used during the first year of mining. As a result, much roof debris fell to the floor in the mains entries/crosscuts off the slope bottom. The roof and ribs were wet, and the debris on the floor was wet and very slippery. In the second summer, the mine installed and operated air conditioning from May to September and the humidity was set at 55%. The entry including the debris on the floor was dry. Little new debris fell from the roof.

B. Leave a top coal

The easiest way to protect the roof shale from weathering is to leave a top coal 6-12 in. (152.4-304.8 mm) thick. The top coal will prevent the ventilation air from contacting the immediate roof shale. The biggest problem with this method is maintaining consistent thickness of top coal during the continuous miner's cutting. A coal-rock interface sensor, such as a gamma ray sensor, must be installed in the continuous miner to measure and maintain a constant top coal thickness. Another constraint is that for low coal seams, it may not be feasible to leave top coal such that the final mining height is below the operating height of the face equipment.

If a top coal layer is used to protect the immediate roof shales, fully grouted resin bolts must be used. If mechanical bolts are used, the gap between the smooth bar and the wall rock allows the air to come in direct contact with the roof strata. In such case, the shale will take on moisture and generate swelling pressure, causing the roof to be unstable.

C. Sealing of rock surfaces and ribs

Another method of preventing roof shales from exposure to the ventilation air is to spray a coat of sealant on the roof and ribs of the entries/crosscuts. To maximize and maintain the bond

between the sealant and roof rock and coal ribs, scaling and thorough cleaning of ribs and roof rock are needed (Pappas et al., 2002; Pritchard et al., 1999). The application process and immense surface areas in underground entries/crosscuts make this method very expensive.

10.6 FLOOR HEAVE

10.6.1 Definition

Floor heave refers to either breaking or lifting up of immediate floor strata, or extrusion of floor strata into entry/crosscut. Floor heave may range from barely visible to fully filling up the entry/crosscut. Floor heave, in most cases, is time-dependent and often occurs in the presence of water.

Floor heave associated with soft floor is fairly common in the eastern coalfield. In the central coal field, due to thick underclay, floor heave is a serious problem. In the western coalfield, thick, hard floor strata are a common feature and rarely present floor problems, though a few exceptions have been reported (Aggson, 1979b; Agapito et al., 2005).

10.6.2 Failure Modes of Floor Heave

Floor failure under a pillar foundation can be divided into three distinct zones (Carpenter and Stephenson, 1978) (Fig. 10.6.1): active zone (zone I), radial shear zone (Zone II), and passive zone (Zone III). The limit of zone I (AC) is inclined at $(45^o + \phi/2)$ to the horizontal; the limit of zone III (DE) is inclined at $(45^o - \phi/2)$ to the horizontal. The failure surface varies from an arc for $\phi = 0$ to a logarithm spiral for $\gamma = 0$.

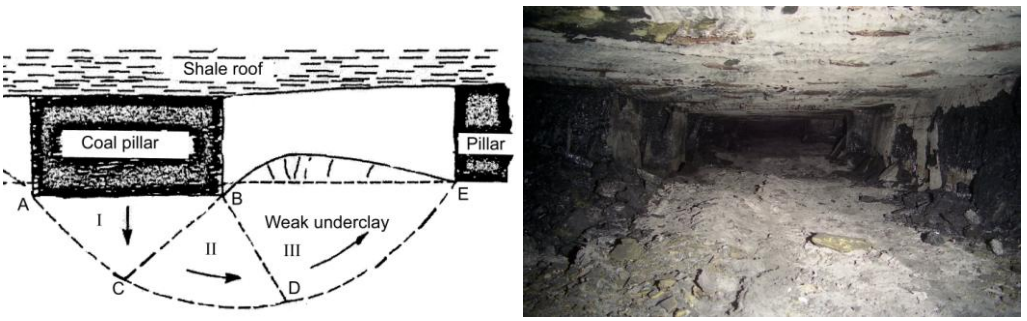

Fig. 10.6.1 General shear failure of floor. Left, Lueckenhoff et al., (1979). Right, Peng, (2007)

Lueckenhoff et al., (1979) investigated through instrumentation the modes of floor failures in four Illinois coal mines and determined that there are three types of coal mine floor failures: general shear failure, pillar punching failure, and beam failure.

General shear failure occurs when the underclay is relatively strong, but the pillar is too small, thereby overstressing the floor. The result is the development of a shear zone, causing the material under the pillar to move laterally toward and then up into the entry/crosscut. The floor bulges in the entry/crosscut. In a **general shear failure**, the slip surface has reached the floor of the entry/crosscut, while in a **local shear failure**, the slip surface does not continue to reach the surface of the entry/crosscut floor (Fig. 10.6.1). In general, shear failure floor heave may be accompanied by pillar sloughing (Peng 1986).

Pillar punching occurs when the floor is thick and relatively soft or becomes soft in the presence of water. In **pillar punching**, failure occurs along the edges of the pillar without the formation of a full failure surface. Cracks develop at the intersection of floor and pillar, and heaved material continues to build up as the pillar punching continues (Fig. 10.6.2). Floor punching may be uniform all around the four sides (Maleki et al., 1993) and is frequently accompanied by pillar sloughage (Fig. 10.6.2).

Beam or buckling failure occurs when the immediate floor is hard, or when a hard floor is relatively shallow and underlain by a soft stratum. As the pillar loads are transmitted through the hard strata to, and sufficient to cause failure of, the soft strata below, the softer materials are displaced upward and outward from beneath the pillar. As this upward and outward movement continues to develop, the hard strata above will eventually buckle and fail in tension (Fig. 10.6.3).

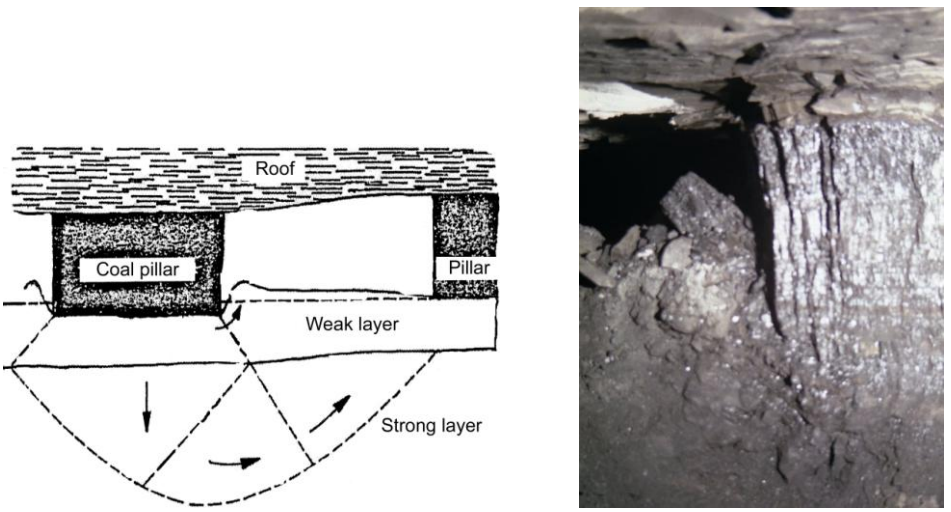

Fig. 10.6.2 Pillar punching of floor failure. Left, Lueckenhoff et al., (1979). Right, pillar punching accompanied by pillar spalling (Peng, 2007; Peng and Wang 1996)

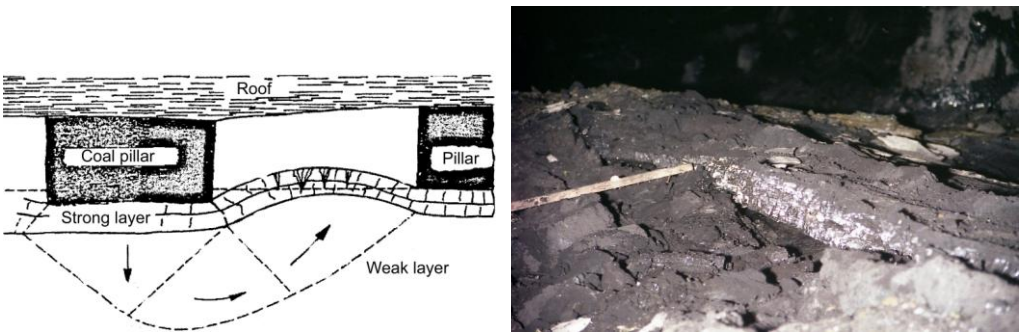

Fig. 10.6.3 Beam failure of floor. Left, Lueckenhoff et al., (1979). Right, Peng (2007)

10.6.3 Bearing Capacity of Floor

Many formulae have been developed for determining foundation bearing capacity in civil engineering (Hans, 1975). However, those formulae were not readily applicable for underground coal mine conditions.

After investigation of floor heave problems in Illinois coal mines, Speck (1981) modified the bearing capacity equation proposed by Vesic (1975) as follows,

$$H_f = \frac{\sigma_{ubc}}{\sigma_v} \tag{10.6.1}$$

$$\sigma_{ubc} = N_{mu}\,(2{,}070 - 167\,C_{wc})\,R \tag{10.6.2}$$

where σ_{ubc} is ultimate bearing capacity, H_f is heave factor. A heave factor less than 1.0 indicates a potentially unstable floor, while a heave factor $\geq$ 1.0 indicates a potentially stable mine floor. σ_v is overburden stress, C_{wc} is natural water content of the floor in percent, R = 0.15 is reduction factor, N_{mu} is a modified bearing capacity factor considering parameters such as,

$$N_{mu} = \frac{rN_c^*\left(N_c^* + \beta_h - 1\right)\left[(r+1)\left(N_c^*\right)^2 + (1 + r\beta_h)N_c^* + \beta_h - 1\right]}{\left[r(r+1)N_c^* + r + \beta_h - 1\right]\left[\left(N_c^* + \beta_h\right)N_c^* + \beta_h - 1\right] - \left(rN_c^* + \beta_h - 1\right)\left(N_c^* + 1\right)} \tag{10.6.3}$$

and r is the strength ratio of the two floor strata, or

$$r = \frac{248}{0.15(2070 - 167C_{wc})} \tag{10.6.4}$$

where 248 is 60 % of the average cohesive strength of claystone (psi), N^*_c is equivalent to Vesic's N^*_c= 6.17, β_h = $P/4H$ is equivalent to Vesic's β term, P is pillar width in feet, and H is thickness of the floor strata.

Based on plate bearing and borehole shear tests over seven coal mines in Illinois where thick soft floor under Herrin #5 and #6 seams is very common, regression equations were developed by Chugh (1986b), Chugh et al., (1989) and Pula et al., (1990) for estimating the ultimate bearing capacity (UBC) and the modulus of deformation at 50 percent, E_{50}, of the UBC. Their studies employed a small test plate varying in size between 36 in^2 and 1 ft^2 (645 mm^2 and 0.093 m^2). They recommended that the following equations can be used during the pre-mining exploration stage:

$$\sigma_{ubc} = 7.38 - 0.145C_{wc} \tag{10.6.5}$$

or

$$\sigma_{ubc} = 1405 - 86C_{wc} - 1.92C_L \tag{10.6.6}$$

$$E_{50} = 5.3x10^4\,C_{wc}^{-0.468} \tag{10.6.7}$$

where σ_{ubc} is the ultimate bearing capacity (UBC) in psi; C_{wc} is moisture content in percent, and C_L is the average liquid limit for weak floor strata down to a depth of 12 in. (0.3 m) below the coal seam.

When the floor is a weaker fireclay underlain by a stronger fireclay at a shallow depth (Su et al., 1993), the failure surface at ultimate load will pass through both layers. When H, the thickness of the weaker layer, is larger than B, the width of the test plate (or pillar width or shield base plate), the failure surface at ultimate load will reside only in the weaker layer. The ultimate bearing capacity under this condition is (Meyhof and Hanna, 1978):

For dry fireclay

$$\sigma_{ubc} = \sigma_{ubst} + \left(\sigma_{ubcb} - \sigma_{ubst}\right)\left(1 - \frac{H}{2B}\right)^2 \geq \sigma_{ubct} \tag{10.6.8}$$

For saturated fireclay

$$\sigma_{ubc} = \sigma_{ubst} + \left(\sigma_{ubcb} - \sigma_{ubst}\right)\left(1 - \frac{H}{B}\right)^2 \geq \sigma_{ubct} \tag{10.6.9}$$

where σ_{ubc} is the ultimate bearing capacity for a given test plate, σ_{ubst} is the ultimate bearing capacity for a given test plate if the weaker fireclay extends to infinity, σ_{ubcb} is the ultimate bearing capacity for a given test plate if the weaker fireclay is not present and the stronger fireclay becomes the immediate floor, and H is thickness of the weaker fireclay.

If the immediate floor is a thin but strong stratum underlain by a weak one, e.g., a floor coal over a thick fireclay, the applied load is spread more uniformly over a large area that reduces the bearing pressure on the weaker stratum thereby increasing the bearing capacity of the weak fireclay.

The floor bearing capacity of fireclay measured by Su et al., (1993) showed that under ambient moisture conditions, the observed floor bearing capacity ranged from 550 psi (3.8 MPa) to 2,083 psi (14.4 MPa). Wetting of the fireclay reduced its bearing capacity by almost 70%. The bearing capacity decreases as the thickness of fireclay increases. Figure 10.6.4 summarizes the test results of bearing capacity of gray fireclay under dry (moisture content = 7.5%), wet (moisture content = 19 %), completely saturated (moisture content = 28.5 %, σ_{ubc} = 322 psi or 2.22 MPa and using Equation 10.6.9), and worst case conditions (σ_{ubc} =0 and using Equation 10.6.9) under various *H/B* ratios.

An example of assessing the base plate toe pressure of a two-leg shield with a floor contact area of 22 in. (0.6 m) wide by 90.5 in. (2.3 m) long is shown in Fig. 10.6.4. Assuming a triangular stress distribution under the base plate, when moisture content is less than 7.5%, the factor of safety for the bearing capacity of the support base plate is always greater than 1.0, i.e., greater than the estimated maximum toe pressure at support yield and setting pressures regardless of gray fireclay thickness (Peng, 2006). The factor of safety will be less than 1.0 if the fireclay thickness is greater than 2.5 ft (0.76 m). Therefore, in order to prevent the shield base plate from punching into the wet floor, the fireclay thickness should be less than the critical thickness of 2.5 ft (0.76 m). Conversely, under completely saturated conditions, or the worst case scenario, the critical fireclay thickness for the base plate employed was about 1 ft (0.3 m).

Utilizing the Hoek-Brown strength criterion, Santos and Bieniawski (1989) developed the following floor bearing capacity equation,

$$\sigma_{ubc} = m\sigma_t \left[\left(\frac{1}{2}\sin^2\phi\right) + \sin\phi\right] + \frac{mE_{rt}}{5} \tag{10.6.10}$$

$$\sigma'_{ubc} = \frac{\sigma_{ubc}}{FS} \tag{10.6.11}$$

where σ'_{ubc} is the designed ultimate bearing capacity, σ_t is tensile strength, ϕ is equivalent angle of internal friction, E_{rt} is point of critical energy release, *FS* is factor of safety, m = 0.001 (highly disturbed rock mass) to 25 (hard intact rock), and s = 0 (jointed rock mass) to 1 (isotropic intact rock material).

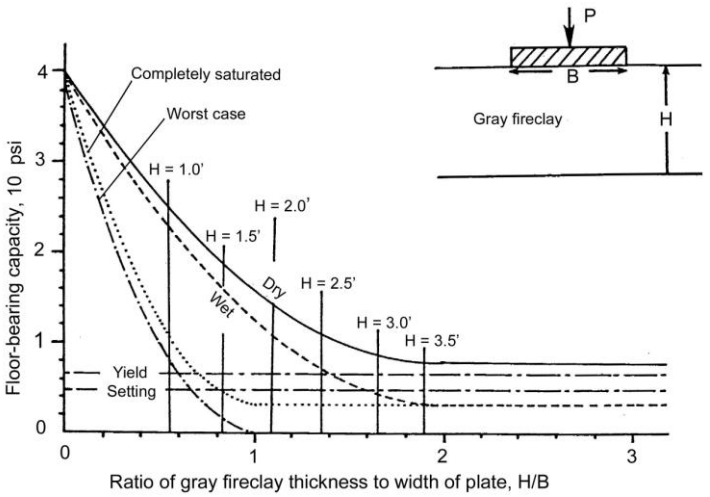

Fig. 10.6.4 Variation of the ultimate bearing capacity with H/B (Su et al., 1993)

10.6.4 Causes of Floor Heave

According to the modes of floor failures, the causes of floor heaves can be classified into the following categories:

1. High Horizontal Stress

High horizontal stress has been attributed to many cases of floor heave (Aggson, 1978a; Jeremic, 1981; Zingano et al., 2002).

Aggson (1978a) studied a case in which the immediate floor, 1 ft (0.3 m) thick, was hard to cut with a continuous miner and subject to high horizontal stresses. The floor buckling tended to occur 2-4 weeks after entry development. Floor buckling occurred as two types: one was a fracture along either side of the ribs with the free end moving up toward the roofline. The other type was fractured at both rib ends and at the entry center, resulting in the floor heave with the entry center higher than both rib ends.

Jeremic (1981) found that the coal floor heaved in different forms depending on the entry orientation with respect to lateral tectonic stress. For a more detailed description refer to Section 6.2.4 (p. 299).

Zingano et al., (2002) found that two factors were responsible for floor heave in a room-and-pillar mine, 98.4 ft (30 m) deep and near the slope of a valley. The two factors were horizontal stress concentration in the immediate floor and the reduction on rock mass strength due to the presence of water.

2. Physical Properties and Occurrence of Floor Strata

The major physical properties that influence the intensity of floor heave are rock type, geological structure, and presence of water (Chugh, 1986a; Wuest, 1992). Soft rocks such as shale and claystone are more susceptible to floor heave. The thicker the soft rock, the more liable it is to floor heave. Nombe and Unrug (2002) found that when the fireclay floor was less than 1.5 ft (0.46 m) thick, the convergence of the floor remained small and therefore, no floor stability problems occurred. The rate of convergence increased when the fireclay was 1.5-2.25

ft (0.46-0.69 m) thick. When the fireclay was greater than 2.25 ft (0.69 m) thick, the total floor convergence was higher, but the rate of convergence diminished.

The thickness and type of immediate and main floors determine the total load the floor can support without failing. In the Illinois coal field, coal seams may be associated with weak immediate floor strata 0.5-8 ft (0.15-2.4 m) thick that are underlain by relatively competent beds, which may have an order of magnitude of higher strength and lower deformability as compared with the weak immediate floor strata.

3. Entry, Pillar and Panel Dimensions

If floor heave is the buckling type, reducing entry width shortens the length of the floor beam that, in turn, will reduce the intensity or possibly eliminate floor heave.

Everything being equal, the larger the pillar width the less stress is imposed on the floor, and consequently, floor heave is less likely. Conversely, a smaller pillar produces higher stress on the floor, so floor heave is more likely to occur. In this respect, pillar design must consider the interaction between roof, coal, and floor.

Finally, coal mine pillars, entries, and crosscuts are laid out in such a way that it must be considered as a 3-dimensional structure. Not only the dimensions of the entries and pillars affect the stress distribution on the floor, panel dimension also controls the stress distribution on the floor. As the panel dimension increases, so does the stress on the floor. When the panel dimension reaches a certain size, producing floor stress larger than the bearing capacity of the floor, floor heave may occur, as shown in case studies by Peng et al., (1995a and 1995b). The same principle applies to massive pillar collapse.

4. Time Factor

It is well known that stresses around mine openings readjust constantly with time to reach a new equilibrium. In the process, rock strength degrades with weathering, and pillar dimension may be reduced from rib sloughage. Case descriptions (Carr et al., 1984; Peng et al., 1995a and 1995b) indicated that floor heave is a time-dependent event. Panel dimension design must take into consideration that the length of time required to mine a panel must be such that panel mining is completed before floor heave becomes a critical factor for production interruption.

5. Water

Presence of water will weaken floor strata, especially clayey materials, contributing to floor heave and massive pillar collapse (Morsy and Peng, 2001 and 2002a). Water also induces stress in the floor strata when confined that may further weaken a weak floor (Tang and Peng, 1991; Peng et al., 1993). In the Pittsburgh seam, the immediate floor in many areas is fireclay, the UCS of which is more than 5,000 psi (34.5 MPa) when dry. But it is reduced to less than 2,000 psi (13.8 MPa) once it is saturated with water. Floor heave does not usually occur during development. During retreat mining a floor may heave up to 2 ft (0.61 m) across the whole entry width and break up near the center, depending on the water saturation condition of the floor and overburden.

The water content of the immediate floor may not be uniform. In the underclay of the Illinois basin, moisture content was about 8 % up to 55 ft (16.8 m) deep and then suddenly reduced to around 4 % and remained so until 140 (m) deep when measurement stopped (Chugh et al., 1987). Vasundhara et al., (2001) dug out a pit to study the characteristics of claystone beneath a long-standing pillar. In roadways, the floor claystone exhibited considerable

swelling, but under the pillars the claystone was very compacted with no open fractures. The edges of the pillar served as the sharp dividing line. The confinement provided by the pillar protected the floor from ingress of moisture and hence from swelling, softening, and weakening. There was no evidence of any plastic flow of floor from under the pillar into the roadways. Floor heave occurred during longwall retreat mining and was measured with associated horizontal extrusion of claystone from beneath the pillar. But the extrusion extended only 3.3-6.6 ft (1-2 m) deep beneath the pillar (Seedsman and Gordon, 1992).

Frequently floor materials involved in floor heave tend to be non-bedded and unconsolidated, containing a lot of slickensides. This type of floor tends to form the general shear type of floor heave (Fig. 10.6.1 right).

10.6.5 Control of Floor Heave

1. Floor Management Program

If the floor is a clayey type of material, it is important to keep the floor dry so that the strength of the floor materials will not deteriorate.

Grading of heaved material can keep roadways clean and open. But roadway grading is non-production time and time-consuming.

2. Slotting in the Floor

Cutting a slot in the floor at the center of the entry can reduce the stress in the floor strata (Aggson, 1978a). In order to be effective, the slot must cut through the thickness of the suspected weak floor layer and be of sufficient width to prevent complete closure.

3. Floor Bolting

Floor bolting, just like roof bolting, has been proven effective to control floor heave (Smith and Pearson, 1961; Stankus and Peng, 1994) (Fig. 10.6.5). However, in order to avoid damage to rubber-tired vehicles, gravel may need to be spread on the finished floor to cover up the protrusion of bolt heads, mat, etc.

Fig. 10.6.5 Comparison of floor condition between floor-bolted and non-bolted entries (Peng, 2007)

4. Cutting Soft Floor Materials/Leaving of Bottom Coal

If the immediate floor layer is not too thick, it is desirable to cut it out to expose the firmer strata below. Alternatively, a bottom coal of 8-12 in. (203.2-304.8 mm) thick may be left to

protect the soft floor. The problem with leaving bottom coal is that it is difficult to control a consistent bottom coal thickness due to operational and geological constraints. For low seams, leaving bottom coals may not be feasible.

5. Use of Yield Pillars

For deep mines where the required stiff pillar dimension may be too large to be economical, yield pillars may be used. However, for yield pillars to be successful, the immediate roof strata must be sufficiently strong to span a large roof span. The alternate is to combine yield and stiff (or abutment) pillars in the mine layout, such as the yield-abutment-yield system for longwall gateroad development (Carr et al., 1984).

6. Re-orientation of Entries/Crosscuts

Just like the roof stability analysis, especially if the floor buckling is due to high horizontal stress, reorienting the entry/crosscut direction is desirable. The principle employed is the same as described in Section 6.2 (p. 288) and 6.3 (p. 303).

7. Proper Mine Design

Three-Dimensional mine structural analysis is the most effective way to determine the proper combinations of panel, entry and pillar dimensions, considering all mining and geological conditions, to prevent floor heave (Hoch and Kramer, 1988; Hsiung and Peng, 1987b; Pytel and Chugh, 1989; Y Wang, 1996; Wang and Peng, 1996).